5-2011

Theoretical Approach for Error Estimation of Temperature and Thermal Conductivity in Uranium Dioxide Fuel

Adam John Gerth

Utah State University

THEORETICAL APPROACH FOR ERROR ESTIMATION

OF TEMPERATURE AND THERMAL CONDUCTIVITY

IN URANIUM DIOXIDE FUEL

by

Adam Gerth

A report submitted in partial fulfillment
of the requirements for the degree

of

MASTER OF SCIENCE

in

Mechanical Engineering

Approved:

Dr. Heng Ban
Committee Chairman

Dr. Barton Smith
Committee Member

Dr. Leijun Li
Committee Member

UTAH STATE UNIVERSITY
Logan, Utah

2011

ABSTRACT

Theoretical Approach for Error Estimation of Temperature and

Thermal Conductivity in Uranium Dioxide Fuel

by

Adam Gerth, Master of Science

Utah State University, 2011

Major Professor: Dr. Heng Ban
Department: Mechanical and Aerospace Engineering

The knowledge of in-reactor thermophysical properties of nuclear fuel rods, which are usually composed of uranium dioxide (UO_2) ceramics, is important for the safe design and operation of nuclear power plants. A two thermocouple method can be utilized to determine the thermal conductivity within the fuel rods by measuring rod centerline temperature and cladding temperature. Using this technique, Halden Reactor Project (HRP) has developed a correlation for thermal conductivity of UO_2 as a function of temperature and burnup. This correlation for thermal conductivity was extracted from experimental data based on a constant thermal conductivity assumption of the fuel rod. However, there are no studies to quantify the error in temperature or thermal conductivity due to the constant thermal conductivity assumption, which will help define the error level of the HRP correlation. Therefore, the first objective for this study was to develop a working model to identify the error associated with constant thermal conductivity of UO_2 compared to the variable conductivity mode using the correlation determined by HRP. The second objective was to develop an approach for data processing that could be used to obtain the correct temperature dependent thermal conductivity. These objectives were achieved by finding analytical solutions of the governing equations with constant and variable thermal conductivity.

Two models were developed to characterize the error between the two assumptions of thermal conductivity. The first model generates the temperature profiles and associated errors of the two assumptions by using constant values for burnup, heat generation, and radius of the fuel rods. The second model is used to determine the dependence of error on heat generation and radius values. Discussion on various solution methods is provided. A hypothetical data set was produced in order to show how the HRP data set can be reprocessed to produce a higher order correlation for thermal conductivity. The result shows that there is as much as 12% error in the temperature profile by assuming constant thermal conductivity. Furthermore, the result shows that the HRP correlation contains an error of about 6%. The higher order data processing method developed in this study can be used in processing HRP or future data from reactor experiments. This study quantified the error of the constant thermal conductivity assumption for UO_2 nuclear fuel rods, and provided a useful tool for data processing.

(90 pages)

ACKNOWLEDGMENTS

I would like to first express appreciation to my major professor, Dr. Heng Ban, for challenging my decisions both inside and outside the classroom. His mentoring motivated me to have reasons for the choices I have made, and am still making. Family and friends have also had an impact on my decisions and motivated me every step of the way.

Lastly, I would like to express appreciation to Bre, my fiancée. While I labored to complete my studies, including this report, she supported me and, without my help, literally planned an entire wedding. It is difficult to express in words how much I appreciate the understanding and love she has shown to me throughout this process.

Adam Gerth

CONTENTS

LIST OF TABLES

LIST OF FIGURES

NOMENCLATURE

A	constant of integration
B	constant of integration
T_0	fuel centerline temperature
k	thermal conductivity
k_0	thermal conductivity at fuel centerline
D	constant of integration
E	constant of integration
k_{Kir}	thermal conductivity constant for Kirchoff Transformation
Ψ	transformation variable for Kirchoff Transformation
α	coefficient of thermal expansion
ρ	material density
c_p	specific heat (constant pressure)
q'''	heat generation rate
r	independent global variable (radial direction)
θ	independent global variable (angular direction)
z	independent global variable (axial direction)
t	independent global variable (time)
T	dependent variable (temperature)
r_s	radial point at surface (cladding) of fuel
T_s	surface (cladding) temperature
O	truncation function (order of dependent variable)
K_s	constant value determined by Kirchoff Transformation

C_1, C_2, C_3	constant values determined by HRP
C_4, C_5	constant values determined by HRP
a	constant values determined by HRP
f, g, h	arbitrary functions
h'	derivative of function h
T_n	new guess value for Newton-Raphson method
T_g	guess value for Newton-Raphson method
$(T,k)_n$	data set of order n
$T_{cons}(r)$	temperature profile solution assuming constant thermal conductivity
$T_{Kir}(r)$	temperature profile solution assuming HRP model
ΔT	temperature difference between centerline and surface of fuel rod
k_n	model for thermal conductivity of order n

CHAPTER 1

INTRODUCTION

Uranium dioxide (UO_2) ceramics are the most common type of nuclear fuel in commercial reactors [1]. The shape and size of the fuel vary depending upon reactor design; however, in general, the shape of the fuel can be described as a long cylinder. A cladding layer of Zircaloy-4 surrounds the fuel to prevent coolant contamination. The temperature difference between the fuel centerline and the cladding can be very large (> 1000°C) which results in high temperature gradients within the fuel rod. Thermal conductivity is an important thermosphysical property because it governs the temperature distribution inside the fuel, which impacts the operational safety of the reactor.

Measurement techniques have been developed to measure properties such as thermal conductivity within the fuel rods [2]. In most cases, a two thermocouple method was used for determining thermal conductivity [3]. This method determines the thermal conductivity by first determining temperature values at the centerline of the fuel and the cladding. Effective thermal conductivity can then be back-calculated from this data. In-pile thermal conductivity measurements are done at the Halden Boiling Water Reactor (HBWR) [4, 5]. The Halden Reactor Project (HRP) determined a correlation for thermal conductivity of UO_2 fuel as a function of fuel burnup and temperature. Uniform fuel composition and density, minimal gap conductance effects, and uniform heat generation within the fuel were assumed to produce this correlation.

Currently, there are no studies to determine the error, or difference, between temperature profiles for the constant thermal conductivity assumption and the HRP expression of UO_2 fuel. There is also no method to obtaining higher order correlations for thermal conductivity. Quantifying the error can aid future designs and models to determine when the centerline temperature has reached a maximum point [6,7]. This study quantifies the error associated with the constant thermal conductivity assumption and also outlines a higher order data processing method for the two thermocouple technique.

This project is intended to quantify the error in the constant thermal conductivity approximation by theoretical analysis. The solutions of the temperature profiles for the constant thermal conductivity assumption and the HRP correlation can be found analytically. By using these analytical solutions, the error in the temperature profile can be determined, as well as the error in the thermal conductivity correlation determined by HRP.

CHAPTER 2

LITERATURE REVIEW

2.1 Thermal Conductivity and Geometry

The ability to properly measure thermal conductivity is important for identifying when temperature limitations of various materials have been reached. Surveys of some of these methods are contained [8-10]. More recently, in-pile measurements have been obtained, which more accurately measure thermal conductivity.

In order to provide useful information in this subject, it is necessary to determine the bounds of the model used to solve for thermal conductivity. Typical limits for commercial reactors are listed in Table 2-1. This information, particularly the maximum fuel centerline temperature, becomes useful in setting up bounds for a temperature profile model.

Table 2-1. Typical Commercial Reactor Fuel and Cladding Parameters [11]

Parameter	Reactor Type	
	PWR	BWR
Fuel		
Material	UO_2	UO_2
Pellet Height	0.6 in (1.5 cm)	0.41 in (1.04 cm)
Pellet Diameter	0.37 in (0.9 cm)	0.41 in (1.04 cm)
Maximum Fuel Center Temperature	3420 ºF (1882 ºC) [12]	3330 ºF (1832 ºC)
Maximum Linear Heat Rate [13]	42.7 kW/m	44.0 kW/m
Average Linear Heat Rate [13]	17.8 kW/m	19.0 kW/m
Cladding		
Material	Zircaloy-4	Zircaloy-2
Outer Diameter	0.422 in (1.07 cm)	0.483 in (1.23 cm)
Thickness	0.024 in (0.06 cm)	0.032 in (0.081 cm)
Average Temperature	657 ºF (347 ºC)	579 ºF (304 ºC)

2.2 A More Accurate Thermal Conductivity Model

The HRP determined by using the two thermocouple method that the thermal conductivity of UO_2 depends on the temperature and burnup of the fuel. The burnup value expresses how much energy the fuel has already produced per mass of UO_2. Their results are summarized in Eq. (1), where the constants are fit parameters determined by the data. Figure 2.1 also shows their graph for thermal conductivity.

$$k(T) = \frac{C_1}{C_2 + aB + (1 - BC_3)T} + C_4 e^{C_5 T} \tag{1}$$

C_1=4040 W/m-K

C_2=464 K

C_3=0.0032 kgUO_2/MWd

C_4=0.0132 W/m-K

C_5=0.00188 K^{-1}

a=16 kgUO_2-K/MWd

This correlation is the most accurate in-pile thermal conductivity correlation for UO_2 fuel available. This correlation allows more exact solutions to be developed for the temperature profile within the fuel. Although being the most accurate available, in order to determine data points, HRP had to assume a constant thermal conductivity profile within the fuel rod. By reprocessing the HRP data, and using the function for thermal conductivity that was determined by HRP instead of the constant thermal conductivity assumption, higher order correlations for thermal conductivity can be determined.

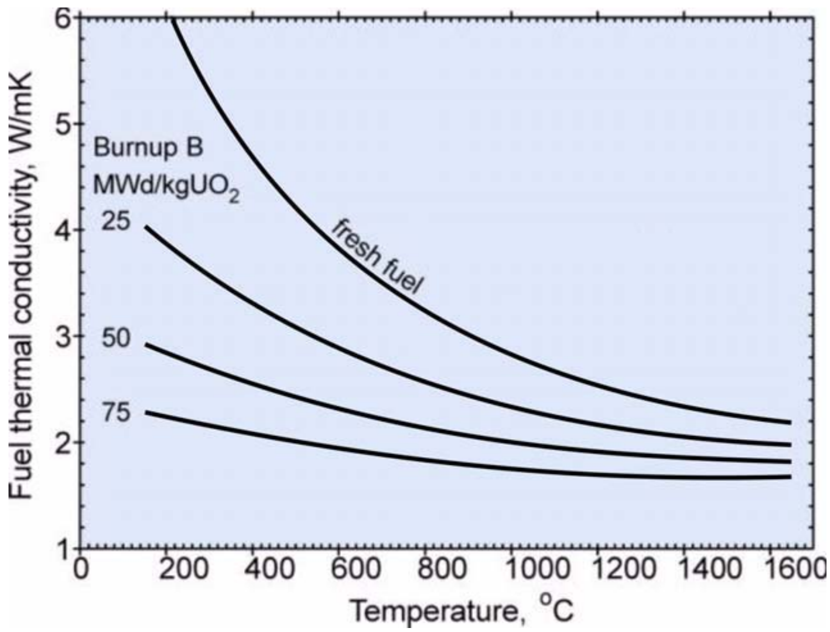

Figure 2-1. HRP measured UO_2 thermal conductivity as a function of temperature and burnup [2].

2.3 Infinitely Long Rod Assumption

For the purposes of this study, one-dimensional (radial) heat conduction is considered. Although, there is heat conduction in the axial direction, in order to utilize the HRP expression for thermal conductivity, the infinitely long rod assumption is carried over from their work.

The two thermocouple method used to produce the HRP expression, is unable to account for axial heat conduction. Experimental modifications to incorporate more thermocouples would resolve this approximation; however, the results would not be general because they would be limited by the specific length of the rod.

2.4 Uniformity Assumption

Although, manufacturing processes, including pressing and sintering, do not guarantee a uniform composition, this model will carry over the HRP assumption that the fuel is compositionally uniform. This affects the directional flow of heat conduction. By using this assumption, the conductance in the angular direction can be neglected. Therefore, the conduction case considered is a radially conducting cylinder.

2.5 Minimal Gap Conductance Effect

This assumption is based on the experimental design of the HRP. The gap effects between the thermocouple probe and the actual fuel was assumed negligible. Because this study is concerned less about the experimental methods used to derive the HRP expression, and more about the inferences from the outcome, there is little that can be done to reject this assumption and thus it is carried over to the analysis of this report.

2.6 Uniform Heat Generation

The HRP expression did not include explanation for the uniform heat generation assumption. The possibility of heat generation being non-constant would have an effect on the governing heat conduction differential equation and may possibly affect the ability to obtain an analytical solution. This would be the case especially if the non-constant behavior was dependent on a parameter other than temperature. Uniform heat generation rate is an assumption used in this study as well.

2.7 Thermocouple Probe Size Neglected

In order to simplify the mathematical expressions for the non-constant property case, the thermocouple probe hole at the center of the fuel was neglected. The size of each thermocouple probe is about 1mm in diameter. The effect this would have on the temperature profile would be to move the centerline boundary condition toward the surface by 0.5mm which is a very small amount. For this purpose, it was assumed that the thermocouple size is negligible.

CHAPTER 3

OBJECTIVES

The objectives of this study are to (1) determine the error in temperature profile , and (2) determine the error in the HRP correlation for thermal conductivity associated with assuming constant thermal conductivity. Accomplishing these objectives necessitates the following tasks:

- Numerically solve the equations for the temperature profiles of the two cases and compare their values. Plot the error in temperature and thermal conductivity as functions of both temperature and radial distance from the fuel centerline.
- Determine how the error changes with fuel radius and heat generation.
- Determine the error of the HRP correlation based on the higher order data processing method.
- Develop a procedure for obtaining the temperature dependent thermal conductivity.

CHAPTER 4

MATHEMATICAL METHODS

4.1 Governing Differential Equation

In order to first determine mathematical solutions, an accurate expression of the phenomena occurring can be expressed in the form of a differential equation. The first equation considered is the heat equation in one dimension for cylindrical coordinates shown by Eq. (2).

$$\frac{1}{r}\frac{d}{dr}\left(rk\frac{dT}{dr}\right) + q''' = 0 \tag{2}$$

Because of the assumption that the rod is infinitely long, the axially conducting term disappears. Also, as a result of uniform heat generation, there can be no gradients in the angular direction so that term can be neglected. Equilibrium is also a condition of this study so the time dependent term is neglected. Equation (3) shows the form of the equation that was solved by HRP.

$$\frac{1}{r}\frac{d}{dr}\left(r\frac{dT}{dr}\right) + \frac{q'''}{k} = 0 \tag{3}$$

This form of the equation is better expressed as the one-dimensional, constant heat generation, steady-state ordinary differential equation for heat conduction in a cylinder. It is important to note that *k*, representing thermal conductivity is constant in this case.

4.2 Solution for Constant Thermal Conductivity

Incropera *et. al* outline a simple method to determine temperature profiles within cylinders for the constant thermal conductivity case [14]. Because the thermal conductivity is a constant in Eq. (3), the differential equation can be solved by integration to obtain Eq. (4), where A and B are constants of integration.

$$T(r) = -\frac{q'''}{4\,k}r^2 + A\ln r + B \tag{4}$$

In order to solve for the constants of integration, the boundary conditions, Eqs. (5) and

(6) are used. The centerline temperature is expressed as T_0 in Eqs. (5) and (6) incorporates the symmetry of the solution from the centerline toward the cladding. It is also important to note that radial distance is measured from the centerline outward.

$$T(0) = T_0 \tag{5}$$

$$\frac{dT(0)}{dr} = 0 \tag{6}$$

In order to ensure that the two thermocouple results are validated, assuming an arbitrary or even scholarly provided thermal conductivity would not be appropriate. The most appropriate number for the thermal conductivity would be a value that allowed the temperatures at both the centerline and the cladding, or fuel surface, to reflect the results of the two thermocouple experiment. Therefore, the solution for this case becomes Eq. (7), where *k*, the thermal conductivity, is still unknown.

$$T(r) = -\frac{q'''}{4\,k} r^2 + T_0 \tag{7}$$

The value for constant thermal conductivity can be determined by using the surface temperature, T_s, as a boundary condition as in Eq. (8).

$$T(r_s) = T_s \tag{8}$$

The expression for thermal conductivity can then be expressed as Eq. (9) and the final solution for the constant thermal conductivity case becomes Eq. (10).

$$k = \frac{q'''\,r^2}{4(T_0 - T_s)} \tag{9}$$

$$T(r) = (T_s - T_0)\left(\frac{r}{r_s}\right)^2 + T_0 \tag{10}$$

4.3 Approximation for Non-Constant Thermal Conductivity Using Taylor Series Method

Jiji has outlined a few methods to deal with the non-linearity that arises in the governing differential equation as a result of non-constant thermal conductivity [15]. One method to obtain the temperature profile is to choose a point, and use a Taylor Series Method to expand infinitely many derivatives out from the point. Theoretically this will map the temperature profile exactly out to any point in the material. The method is summarized in Eq. (11).

$$T(r) = T(0) + \frac{dT(0)}{dr}\frac{r}{1!} + \frac{d^2T(0)}{dr^2}\frac{r^2}{2!} + \frac{d^3T(0)}{dr^3}\frac{r^3}{3!} + \cdots + \frac{d^nT(0)}{dr^n}\frac{r^n}{n!} \tag{11}$$

The first term comes from Eq. (5) and the second term is zero from Eq. (6). We can then develop an expression for the second derivative by manipulating the governing differential equation. By carrying this out, the second derivative at the centerline becomes Eq. (12), where k_0 is the thermal conductivity at the centerline ($k(T_0)$).

$$\frac{d^2T(0)}{dr^2} = -\frac{q'''}{k_0} \tag{12}$$

The third derivative comes by taking the first derivative of the governing differential equation with respect to the radius. This reduces to the relatively simple expression in Eq. (13).

$$\frac{d^3T(0)}{dr^3} = \frac{q'''}{r\,k_0} \tag{13}$$

The fourth and fifth derivatives are quite complex, and so, to save space in this report will not be shown explicitly. However, the fourth and fifth derivatives can be determined by taking the first derivative of the third and fourth derivative expressions, respectively.

The reason this method is an approximation is due to the fact that it is not feasible to carry the terms out to more than about five or six. The mathematics, particularly the chain rule, become very heinous for this case, so five terms is the maximum terms included.

By gathering the derivatives, placing them into Eq. (11), and simplifying, the Taylor Series Approximation of the solution for the temperature profile is given by Eq. (14), with truncation error on the order of r^6.

$$T(r) = T_0 - \frac{43\,q'''}{120\,k_0}r^2 - \frac{q'''}{24\,{k_0}^3}\frac{dk(0)}{dT}r^4 + O(r^6) \tag{14}$$

As will be shown in Chapter 6, as this approximation is extended to the cladding, or surface, it diverges grossly from the actual solution. Therefore, it can be concluded that the first five derivatives do not contain enough information about the actual temperature gradients in the fuel rods.

4.4 Solution for Non-Constant Thermal Conductivity Using Kirchoff Transformation

An analytical solution to the problem can be obtained by using a method known as the Kirchoff Transformation. This technique makes the substitution in Eq. (15) which reduces the non-linear differential equation to a linear one, where k_{Kir} is an arbitrary constant for thermal conductivity.

$$\Psi(T) = \frac{1}{k_{Kir}} \int_0^T k(T)\, dT \tag{15}$$

This substitution allows functions in radial distance and temperature to be separated and equated ($f(r) = g(T)$, where g and f are functions determined by the solution). Based on the substitution in Eq. (15), Eq. (2) becomes Eq. (16).

$$\frac{d}{dr}\left(r\frac{d\Psi}{dr}\right) + \frac{q'''}{k_{Kir}} r = 0 \tag{16}$$

Just as before, Eq. (16) can be solved by integrating twice to obtain Eq. (17), where D and E are constants of integration.

$$\Psi(r) = -\frac{q'''}{4\, k_{Kir}} r^2 + D \ln r + E \tag{17}$$

The boundary conditions in Eqs. (6) and (8) can also be changed using the transformation into Eqs. (18) and (19), where $F(T_s)$ is the integral expression solved in Eq. (15) for T_s.

$$\frac{d\Psi(0)}{dr} = 0 \tag{18}$$

$$\Psi(r_s) = F(T_s) = \Psi_s \tag{19}$$

Incorporating these boundary conditions produces a solution for the transformation variable, Ψ, in Eq. (20).

$$\Psi(r) = \frac{q'''}{4\,k_{Kir}}({r_s}^2 - r^2) + \Psi_s \tag{20}$$

At this point, the substitution in Eq. (11) can be analytically solved because the expression for thermal conductivity is known from HRP results. After accomplishing this for T_s, the expression for Ψ_s is summarized by Eq. (21).

$$K_s = \Psi_s k_{Kir} = \frac{C_1}{1 - BC_3} \ln\{[C_2 + aB + (1 - BC_3)T_s][C_2 + aB]\} + \frac{C_4}{C_5}\left(e^{C_5 T_s} - 1\right) \tag{21}$$

Once again, by solving Eq. (11) for T, the full analytical solution to the non-linear ordinary differential equation can be written as Eq. (22).

$$\frac{C_1}{1 - BC_3} \ln\{[C_2 + aB + (1 - BC_3)T][C_2 + aB]\} + \frac{C_4}{C_5}\left(e^{C_5 T} - 1\right) = \frac{q'''}{4}({r_s}^2 - r^2) + K_s \tag{22}$$

In this form, the ability to analytically solve for temperature is not possible. The next chapter will discuss the numerical approaches to determine the solution.

CHAPTER 5

NUMERICAL MODELING

5.1 Newton-Raphson Method

The form of Eq. (22) demands the use of numerical methods. The simplest method to determine the temperature profile from the analytical solution is the Newton-Raphson root finding method.

Since the solution is of the form $f(r) = g(T)$, by subtracting $g(T)$ from both sides of the equation and letting r be a constant value at some distance from the centerline within the fuel rod, the equation then becomes of the form $h(T) = f(r) - g(T) = 0$. By applying a guess value for temperature, a new guess value can be determined by Eq. (23).

$$T_n = T_g - \frac{h(T)}{h'(T)} \tag{23}$$

The solution is considered converged when the new value for temperature is less than 0.0001% different from the previous guess value. By iterating over the radius of the fuel rod, the temperature profile can be mapped for the Kirchoff Transformation solution.

One particular point of concern comes from determining the initial guess value for the Newton-Raphson method. In order to assure that the computer converges to the correct value for temperature, the initial guess value is always 100 K greater than the centerline temperature.

5.2 Code Instability

Because the Newton-Raphson method relies on the function h and h', it becomes necessary to determine where these expressions take on infinite or imaginary values. The only point in Eq. (23) of possible concern is in the expression for h. There is a natural log term given as Eq. (24).

$$\ln\{[C_2 + aB + (1 - BC_3)T][C_2 + aB]\} \tag{24}$$

The second part of this expression is always a constant positive value (C_2+aB), therefore, the only part of Eq. (24) that needs to be checked is Eq. (25).

$$C_2 + aB + (1 - BC_3)T > 0 \tag{25}$$

By simplifying Eq. (25), Eq. (26) is an expression that must be satisfied every time for T to ensure code stability.

$$T > \frac{C_2 + aB}{BC_3 - 1} \tag{26}$$

This gives a general expression for temperature that is a function of the burnup parameter. By evaluating the expression and recalling the effective temperature range from [11], there becomes a critical value for the burnup parameter. It is clear that as long as the burnup parameter is positive (or analytically B > -77 MWd/kgUO_2), then the code is stable. Therefore, practicality prohibits any code instability.

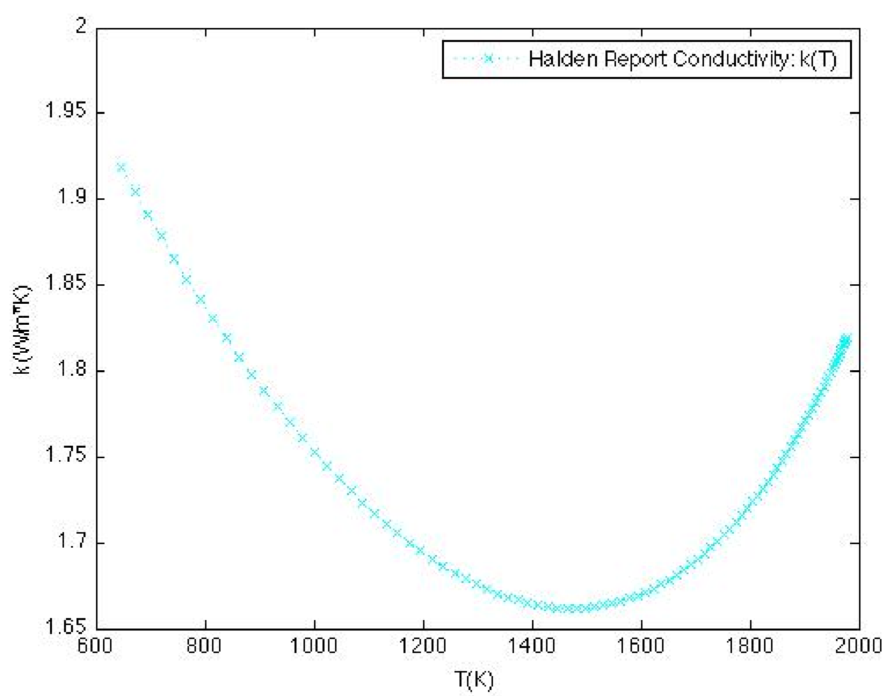

Figure 5-1.HRP thermal conductivity over higher temperature range for B = 75 MWd/kgUO_2.

5.3 HRP Correction

The thermal conductivity expression determined by HRP has one clear point of correction. For higher values of temperature, the graph for thermal conductivity has a pronounced minimum. This presents a topic for discussion (see Figure 5-1).

Under this situation two conclusions could be made. The first conclusion is that the true behavior for thermal conductivity of UO_2 has a pronounced minimum around 1800K. The second conclusion, and more practical, is that the expression given by HRP is only fitted for a smaller range of temperature values and that instead of a minimum, there exists an asymptote.

The second conclusion is has greater likelihood because of the measurement instruments used. The temperature tolerance of the instruments probably did not extend high enough to record higher temperature behavior.

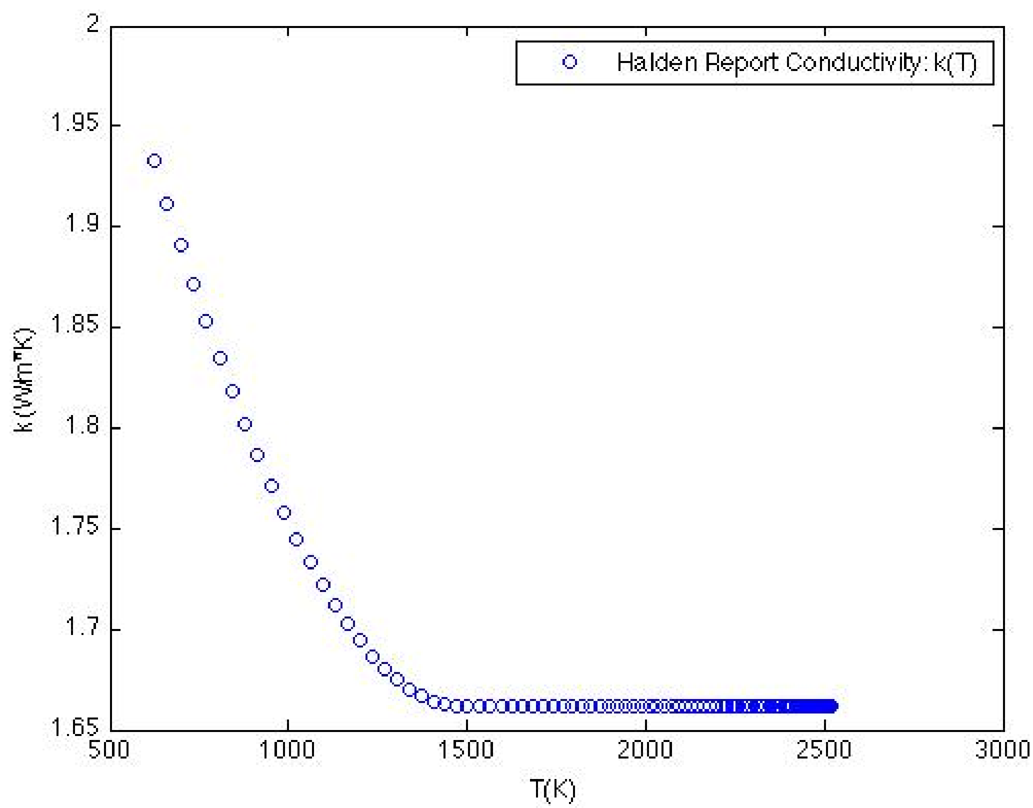

Figure 5-2.Corrected HRP thermal conductivity over higher temperature range for *B* = 75 MWd/kgUO_2.

For the purpose of the model, as soon as the minimum critical value was found, a correction was made. An asymptote formula was used to determine the thermal conductivity at temperature values greater than the critical point (see Figure 5-2).

5.4 Limits of Model

In order to investigate dependence of error on heat generation rate and fuel size it is important to determine the bounds for the model. The heat generation values for the model range from 4E7 BTU/(hr-ft^3) (414 kW/m^3)to 5E7 BTU/(hr-ft^3) (517 kW/m^3). The radius sizes range from 3mm to 10mm, or diameters from 6mm to 20mm.

A further feature of the model is the incorporation of the peak centerline temperature. A maximum temperature of 2106K was used. Any points that determined the centerline temperature to be greater than this were rejected as high out of bound.

CHAPTER 6

RESULTS AND DISCUSSION

This chapter is organized into three sections in order to present the results of the models in a simple manner. The first section, 6.1-6.3, is a discussion on the results for the temperature profiles determined by numerical methods. The error of the constant thermal conductivity assumption within the fuel rod is also discussed. The second section, 6.4, presents results from the second model which determines the maximum error in the temperature profile due to the constant thermal conductivity assumption for various fuel radii and heat generation rates. The third section, 6.5-6.6, is useful for commercial reactors without two thermocouple instrumentation. For various fuel compositions, the best approximation for fuel centerline temperature and constant thermal conductivity are listed based on the HRP correlation and assuming thermal equilibrium.

6.1 Temperature profiles

The temperature profiles for the three cases were considered. The plots developed by the model indicate that the Taylor Series Approximation is not sufficient. Both the constant thermal conductivity solution and the Kirchoff Transformation solution agree at the boundary conditions.

6.1.1 Taylor Series Approximation

The Taylor Series Approximation gave a relatively straight-forward analytical expression for the temperature at any point within the fuel rod. The truncation order was the sixth power of the radial dimension.

The plot of the Taylor Series Approximation shows that this method is inadequate (see Figure 6-1). The Taylor Series Approximation diverges grossly from the other solution methods near the fuel wall (127% difference). Furthermore, this solution produces negative temperatures on the Kelvin scale, which is extremely erroneous (surface temperature: -169K).

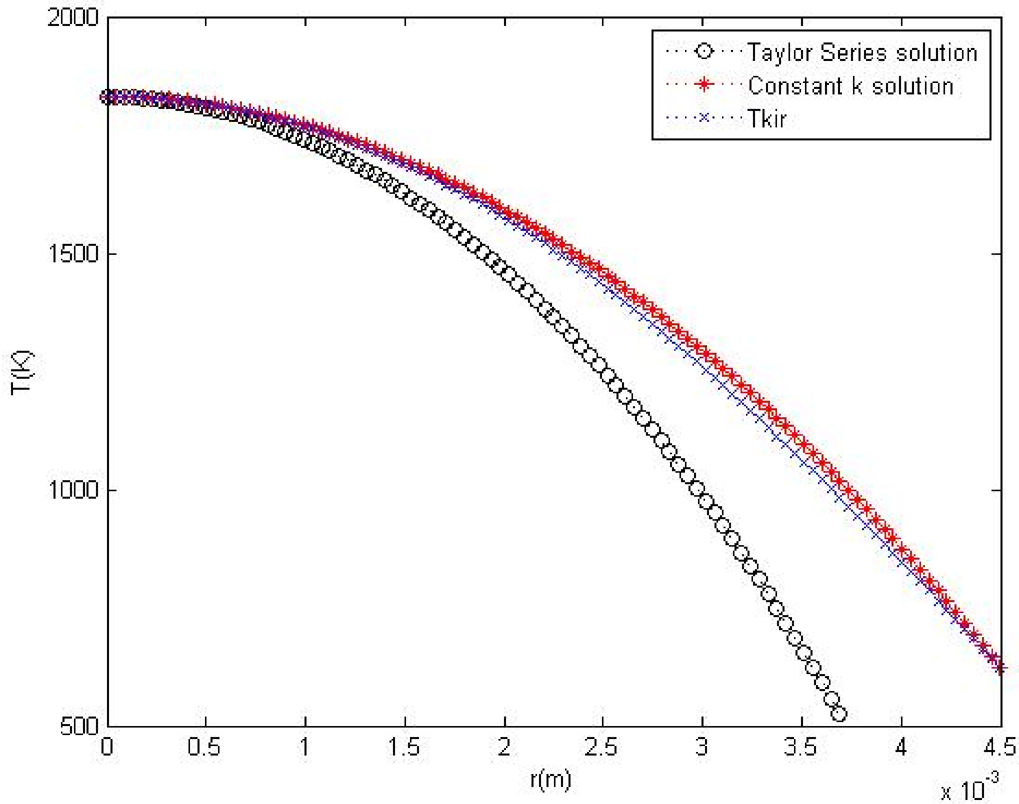

Figure 6-1.Temperature profile solutions for B = 50 MWd/kgUO_2.

The conclusion of this observation is that there is evidence that higher order derivatives affect the solution of the temperature profile. The reason for this may come from the logarithmic and exponential nature of the solution given by the Kirchoff Transformation. This solution case was rejected and will no longer be included in the remainder of the discussion.

6.1.2 Kirchoff Transformation and Constant Thermal Conductivity Comparison

The Kirchoff Transformation and constant thermal conductivity solutions provide analytical solutions to the governing differential equation for the case of the fuel rod. Furthermore, since boundary conditions are incorporated, these solutions converge at the boundaries of the problem (see Figure 6-2).

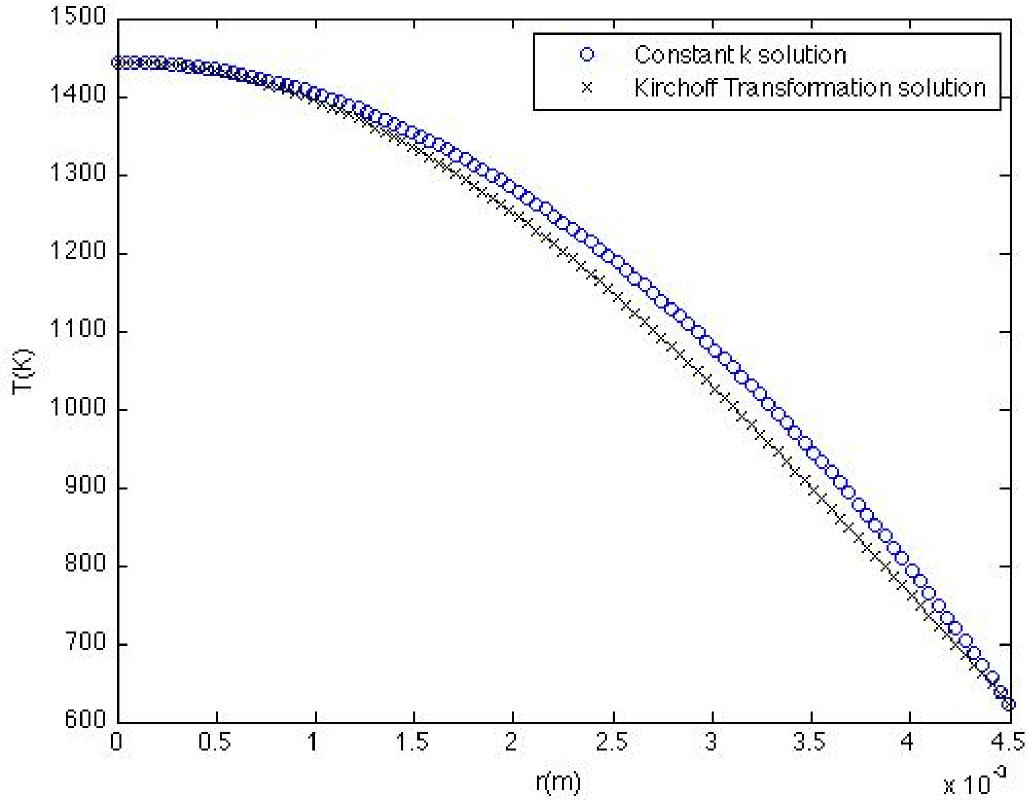

Figure 6-2.Temperature profile solutions for B = 0 MWd/kgUO_2.

At higher burnup rates the plot for temperature even exhibits a common point between the centerline and surface where the two solutions cross each other (see Figure 6-3). This is possibly a result of the higher temperature difference between the centerline and the surface. The plots also seem to have a smaller error between the profiles. This will be discussed in deeper detail later in the report.

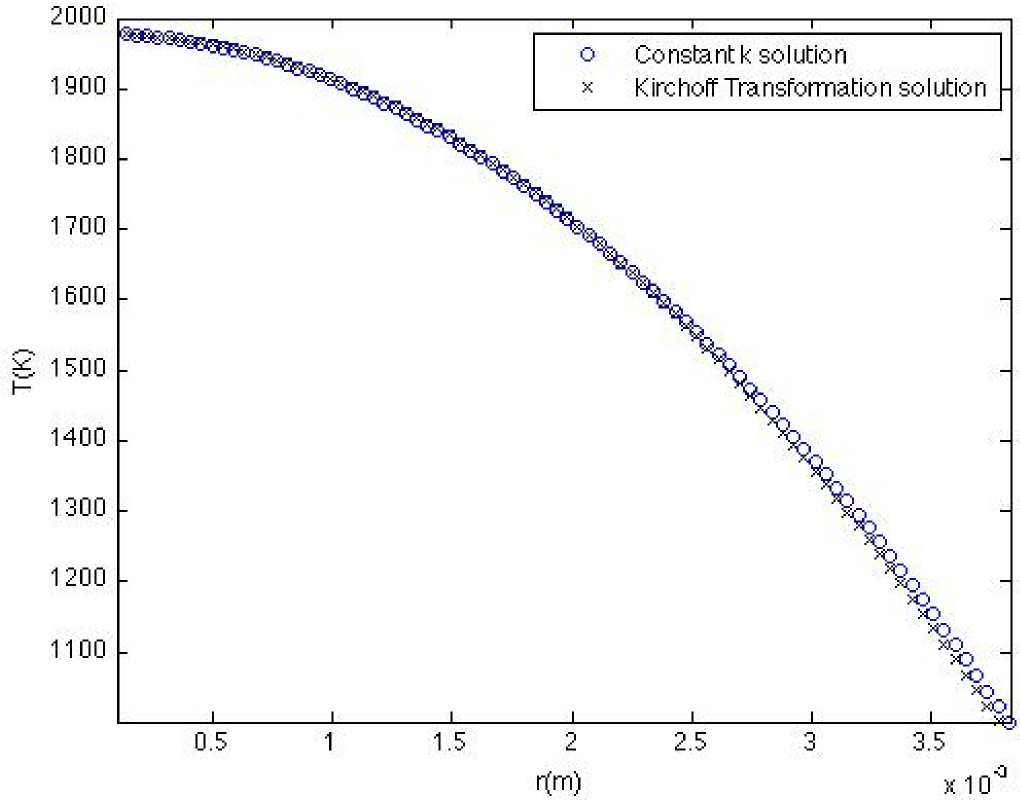

Figure 6-3. Temperature profile solutions for B = 75 MWd/kgUO_2.

6.2 Thermal Conductivity Plots

The Mathematical Methods chapter discusses where the value of thermal conductivity for the constant thermal conductivity solution comes from. This value seems to be roughly equal to the value predicted by HRP at the center of the temperature range for the fuel rod profile (see Figure 6-4).

Another interesting point is where this intersection occurs within the fuel rod. From Figure 6-5, it is apparent that the prediction for constant thermal conductivity matches the correct value near the surface of the fuel rod. Therefore, it seems that the constant thermal conductivity value relies more heavily upon the temperature range than the average in the radial direction.

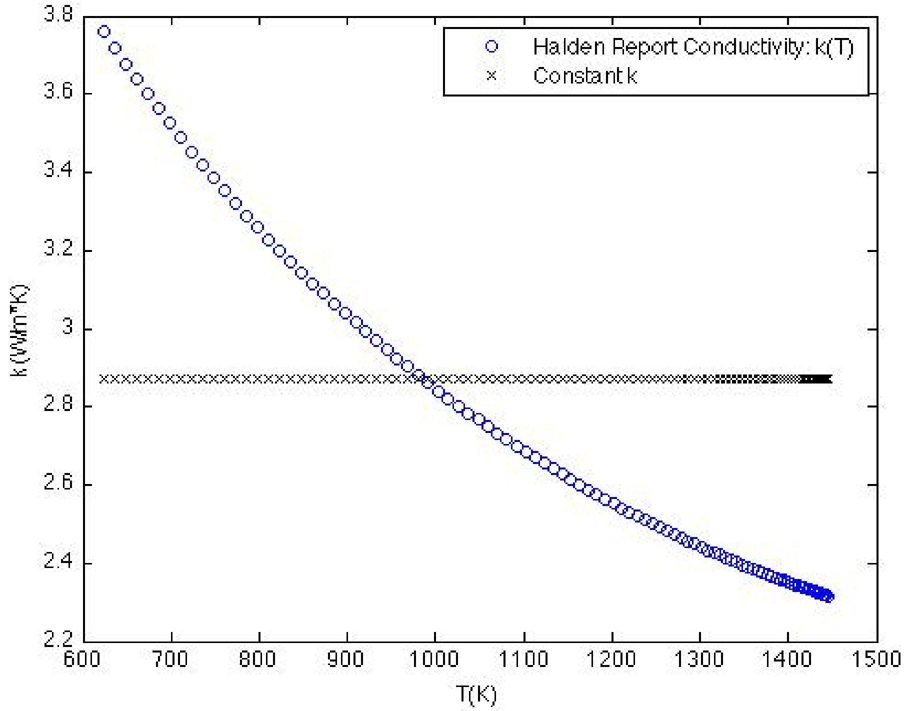

Figure 6-4. Thermal conductivity plot against temperature for B = 0 MWd/kgUO_2.

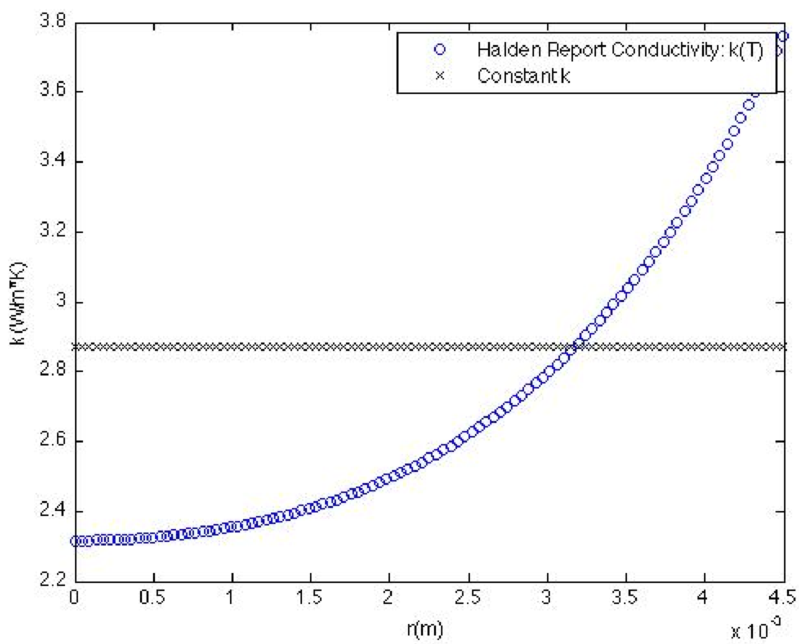

Figure 6-5. Thermal conductivity plot against radius for B = 0 MWd/kgUO_2.

Even more information can be obtained by observing the graphs of fuel with a higher burnup value. The conclusion still holds that the constant value for thermal conductivity depends more on the temperature range than the average in the radial direction. Furthermore, the constant thermal conductivity value is closer to the HRP values at higher burnup rates. This is due to decrease in overall thermal conductivity as the fuel is spent (see Figure 6-6 and 6-7).

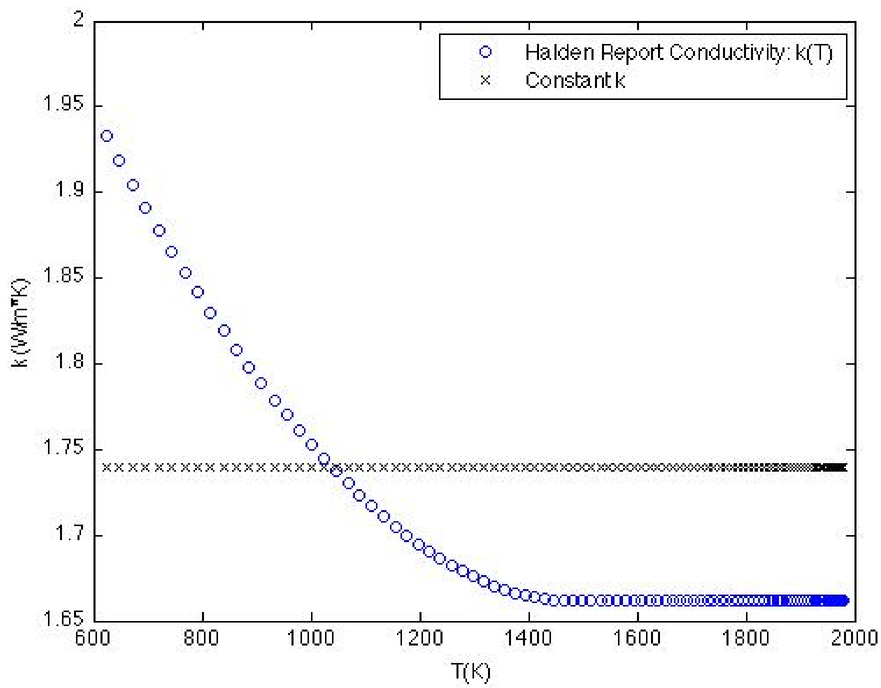

Figure 6-6. Thermal conductivity plot against temperature for B = 75 MWd/kgUO$_2$.

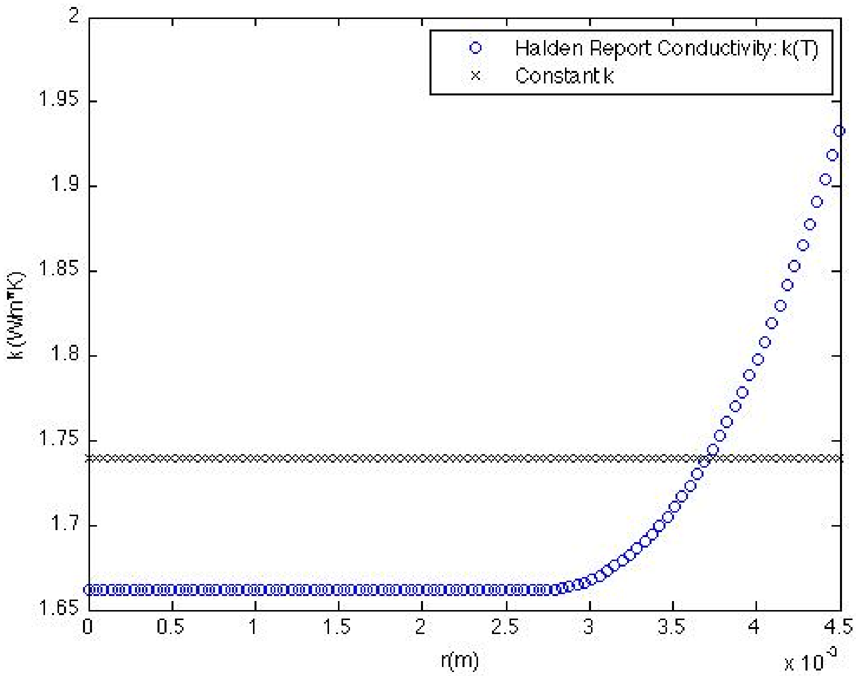

Figure 6-7. Thermal conductivity plot against radius for B = 75 MWd/kgUO$_2$.

6.3 Error Assuming Constant Thermal Conductivity

The error, or difference, between the constant thermal conductivity value and the HRP expression depends on the local temperature. The model was developed in order to get a clear picture of where this error is occurring both on a temperature scale and also geometrically using radius as the independent variable.

6.3.1 Error as a Function of Temperature

The relationship between thermal conductivity error and temperature error is inversely proportional within the fuel rod. When the error for thermal conductivity is experiencing its maximum value in the fuel rod, then the error for temperature is at a minimum, and vice versa. Another conclusion that is clear from prior discussion is that the error for thermal conductivity is only zero at one point, whereas the error for temperature is zero at the boundaries (see Figure 6-8).

The largest error for thermal conductivity occurs at the limits of the temperature range. The greatest value is associated with the error at the lowest temperature limit. This is true because of the asymptotic behavior of the HRP expression.

The temperature profile for the constant thermal conductivity assumption exhibits larger errors at lower temperatures. This is a result of the higher thermal conductivity values at these lower temperatures. Because the gradient becomes steeper, the error increases.

6.3.2 Error as a Function of Radial Position

By using the temperature profile to determine where the temperatures occur radially, the errors can be determined as a function of radial distance. The plot shows similar behavior to the temperature dependent plot, however, the results are skewed toward the surface even more (see Figure 6-9).

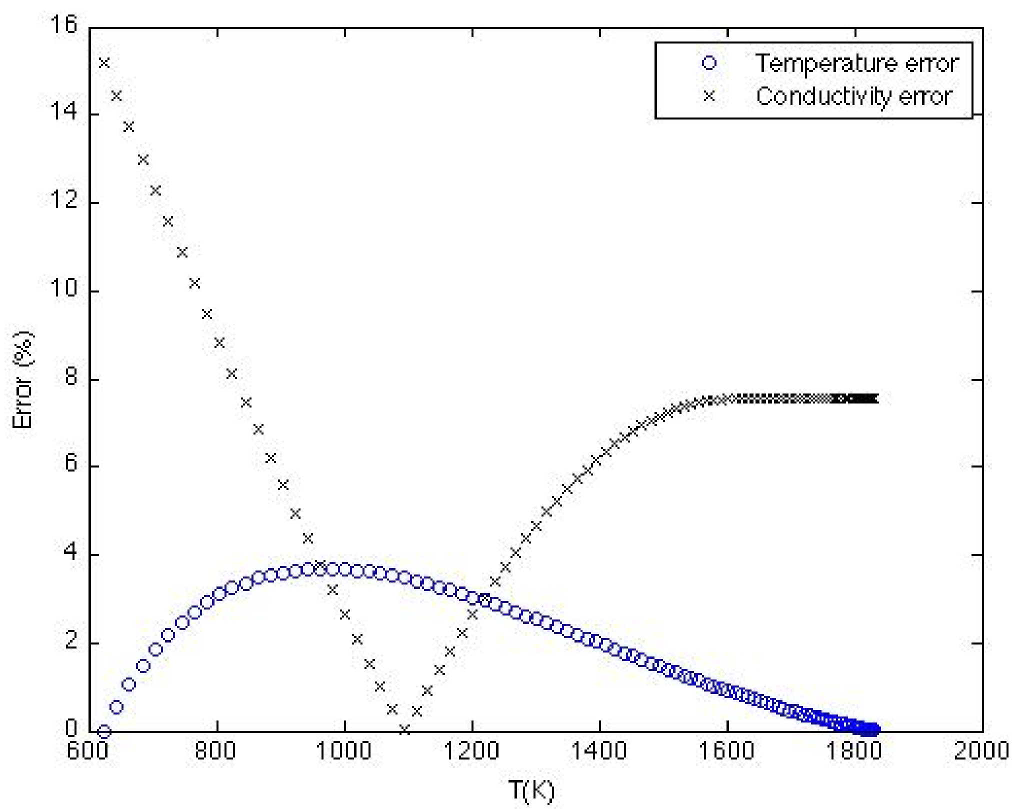

Figure 6-8. Error of constant thermal conductivity assumption against temperature for B = 50 MWd/kgUO$_2$.

At a position that is approximately three-quarters the distance from the centerline to the surface, the constant thermal conductivity value becomes the true value, and the temperature error experiences its greatest error. Once again, the greatest error for thermal conductivity occurs at the surface of the fuel rod.

The temperature error is of some significance. This plot shows that the error in temperature over the radius is relatively small compared to the maximum error in temperature (~4%). If these results are to be used for correction of thermal expansion, then the correction does not need to be large.

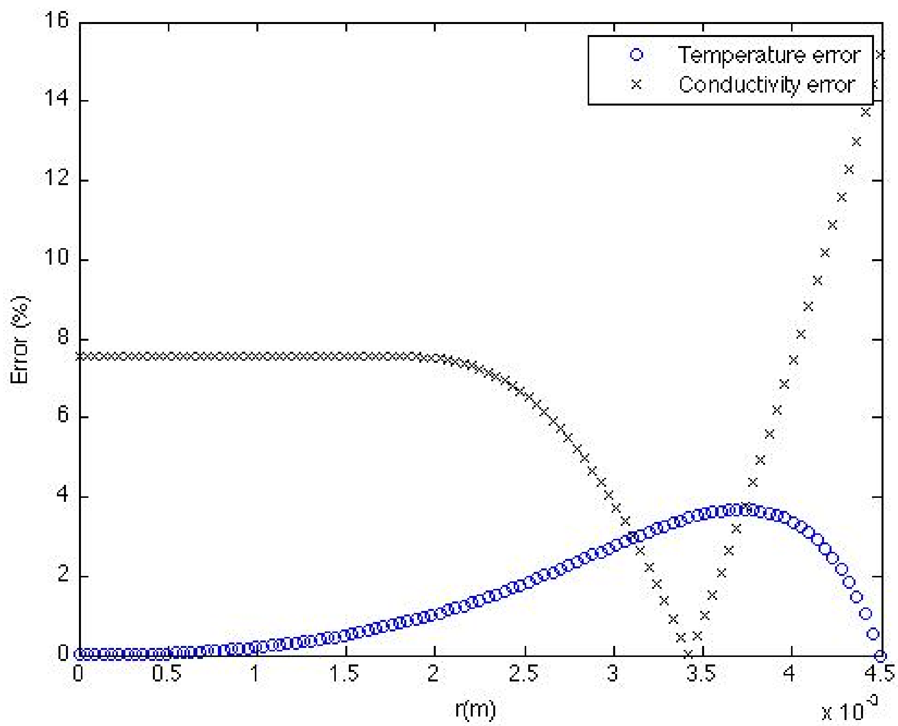

Figure 6-9. Error of constant thermal conductivity assumption against radius for B = 50 MWd/kgUO_2.

6.3.3 Error as a Function of Burnup

The burnup value seems to play an important role in contributing to the error of the constant thermal conductivity assumption. For one case, the temperature profile error was shown to be ~12% for a burnup value of 0 MWd/kgUO_2 (see Figure B-1). At higher burnup values, because the error in thermal conductivity is smaller, the error in the temperature profile is also smaller for a given point in the fuel rod (see Figure 6-10 and 6-11). Therefore, as core life increases, the ability to predict the temperature profile by using the constant thermal conductivity assumption improves.

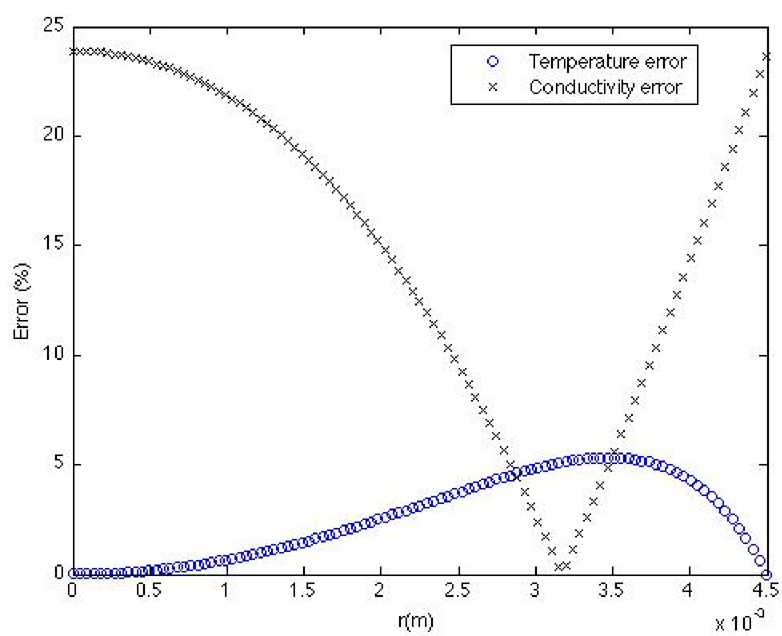

Figure 6-10. Error of constant thermal conductivity assumption against radius for B = 0 MWd/kgUO_2.

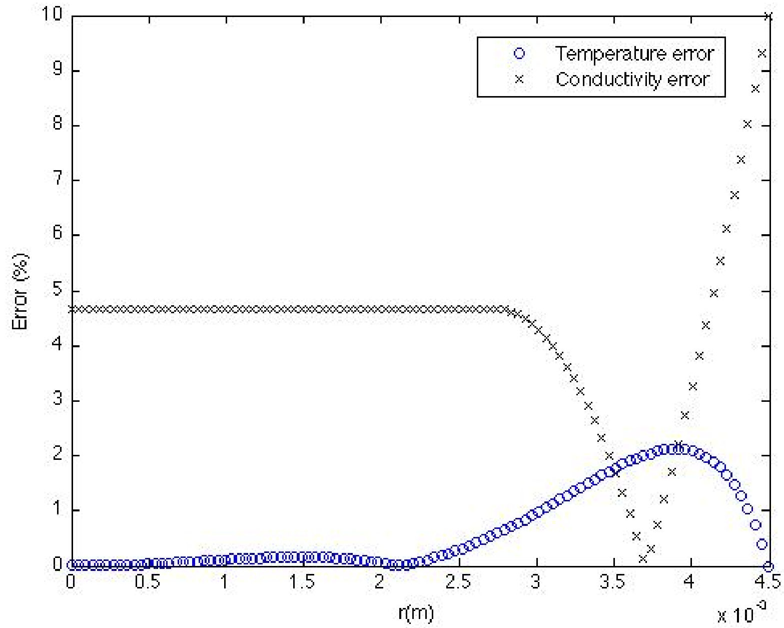

Figure 6-11. Error of constant thermal conductivity assumption against radius for *B* = 75 MWd/kgUO_2.

6.4 Error Dependence on Heat Generation and Fuel Size

After knowledge of the above error profile has been obtained, the maximum error can be used to determine the error dependence on fuel parameters such as heat generation rate and diameter. As mentioned, the maximum values for error occur at different points for thermal conductivity and temperature.

By using the limits discussed in the Numerical Modeling Chapter, the error profile problem can be solved iteratively for various values of heat generation rate and radius. The points that are plotted represent the maximum errors for the various error profiles (see Figure 6-12).

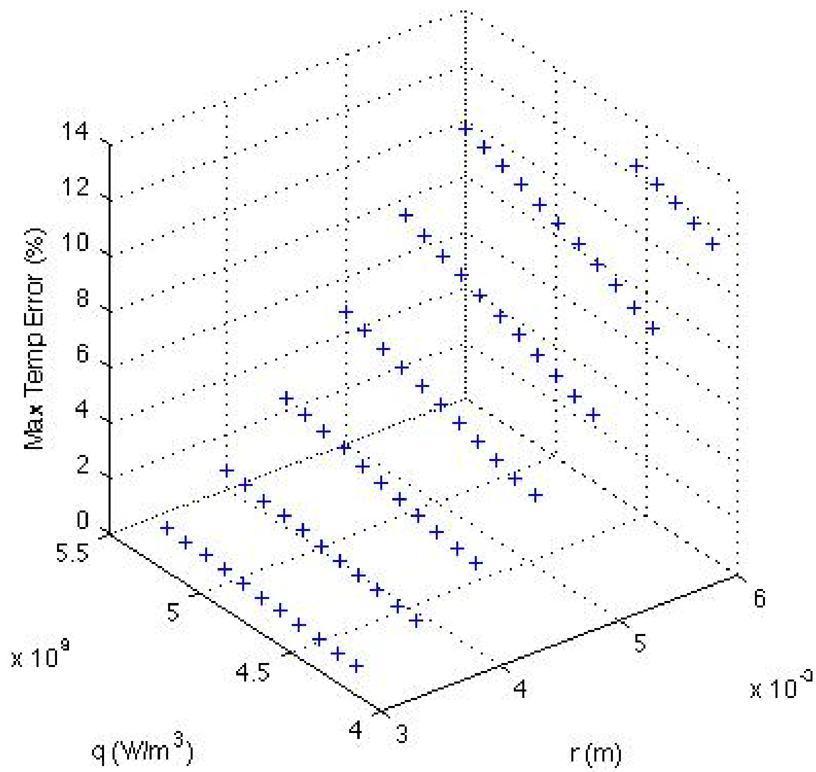

Figure 6-12. Error of constant thermal conductivity assumption for B = 0 MWd/kgUO$_2$ for various heat generation rates and fuel sizes.

The trend in temperature error seems to be somewhat upward with both heat generation rate and radius of the fuel. This is also true for the thermal conductivity error. The three dimensional plot makes it difficult to determine actual dependence on one variable or the other. By rotating the plot, to show the error as a function of one axis, better conclusions can be determined.

The first conclusion is that the error has relatively small dependence on heat generation rate. Although there is a slight trend for a given value of heat generation rate, the range of the error is quite large (see Figure 6-13). This suggests that the partial effect of heat generation does not contribute as much to the error as other parameters. The small dependence that there is seems to suggest that as heat generation rate increases, the maximum error of the constant thermal conductivity assumption also increases.

The second conclusion comes by rotating the picture to the radius axis. This view shows that the partial effect of radius contributes a lot more to the maximum error of the constant thermal conductivity assumption. The range of error values for a given radius suggests that there is a relatively small interaction between fuel radius and heat generation rate, but that the error is impacted more by the radius (see Figure 6-14).

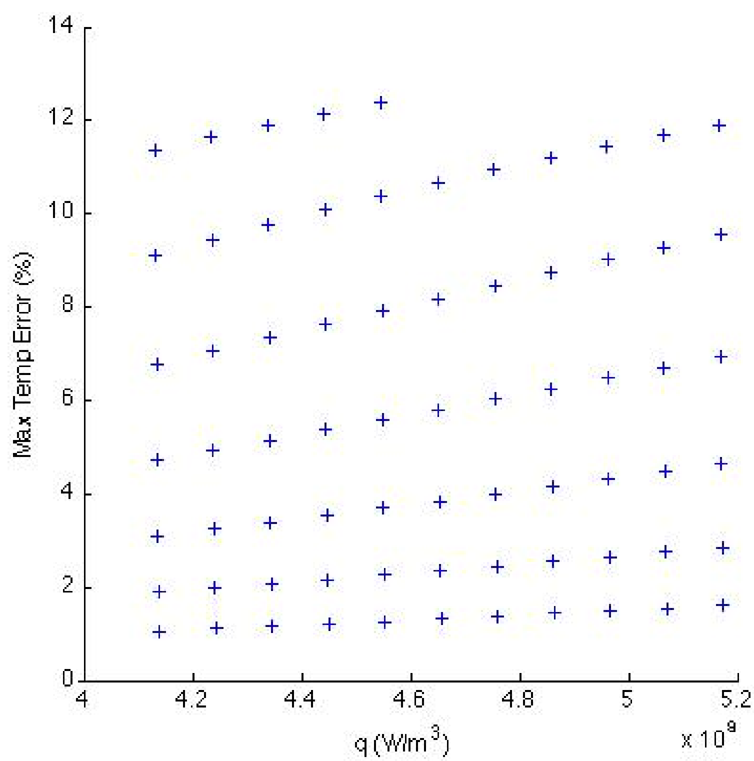

Figure 6-13. Error of constant thermal conductivity assumption for $B = 0$ MWd/kgUO$_2$ against heat generation rate.

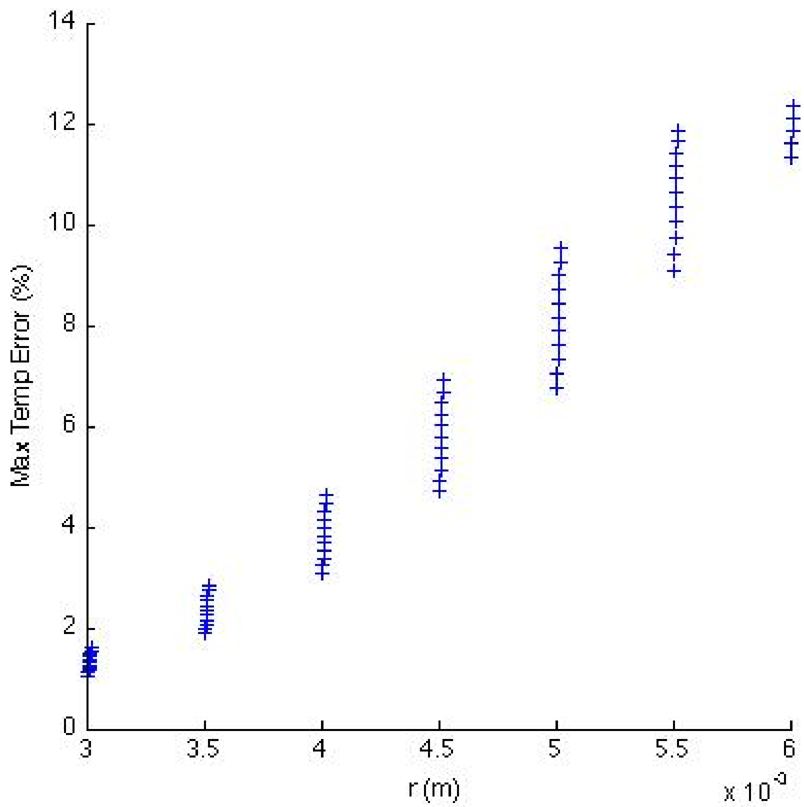

Figure 6-14. Error of constant thermal conductivity assumption for $B = 0$ MWd/kgUO_2 against fuel sizes.

In conclusion, the main effect that contributes to the error is the fuel radius. There seems to be a small interaction between radius and heat generation rate that is evident by the range of maximum error values for a given radius. The heat generation rate alone does not seem to have a very significant impact on the maximum error other than its contribution when interacting with the fuel radius.

6.5 Determining Fuel Centerline Temperature

More information is available from the model. In order to solve the temperature profile, the fuel centerline temperature has to be determined. In practical application, this value is important for the safety and operation of nuclear reactors. Based on the HPR results, this value can be determined for various fuel sizes, heat generation rates, and burnup values. The following are tables displaying this temperature for different burnup values. It is important to note that in the model, all cases where this temperature was greater than 2106K were rejected because of typical operating limits. The values were also determined based on thermal equilibrium and a surface temperature of 623 K.

Table 6-1. Centerline Temperature for $B = 0$ MWd/kgUO_2

$B = 0$ MWd/kgUO_2								
Centerline Temp. (K)		Fuel radius (mm)						
		3	3.5	4	4.5	5	5.5	6
q''' (MW/m^3)	414	809	917	1052	1219	1421	1662	1935
	424	816	928	1067	1240	1449	1698	1977
	435	824	938	1082	1261	1477	1733	2020
	445	830	949	1098	1282	1505	1769	2062
	455	838	960	1113	1303	1534	1805	2103
	466	846	971	1129	1325	1563	1841	X
	476	853	982	1144	1346	1592	1877	X
	486	860	993	1160	1368	1621	1913	X
	497	868	1004	1176	1390	1650	1949	X
	507	875	1015	1192	1413	1680	1985	X
	517	883	1027	1209	1435	1709	2020	X

Table 6-2. Centerline Temperature for B = 25 $MWd/kgUO_2$

B = 25 $MWd/kgUO_2$							
Centerline Temp. (K)		Fuel radius (mm)					
		3	3.5	4	4.5	5	5.5
q''' (MW/m^3)	414	894	1035	1208	1417	1661	1933
	424	904	1049	1227	1443	1694	1972
	435	913	1063	1247	1468	1726	2010
	445	923	1077	1266	1494	1759	2047
	455	933	1091	1286	1520	1791	2085
	466	942	1105	1305	1546	1824	X
	476	952	1119	1325	1572	1856	X
	486	962	1133	1345	1598	1888	X
	497	971	1147	1364	1625	1920	X
	507	981	1161	1384	1651	1952	X
	517	991	1176	1404	1677	1984	X

Table 6-3. Centerline Temperature for B = 50 MWd/kgUO_2

B = 50 MWd/kgUO_2						
Centerline Temp. (K)		Fuel radius (mm)				
		3	3.5	4	4.5	5
q''' (MW/m^3)	414	977	1147	1353	1594	1862
	424	988	1164	1375	1622	1896
	435	1000	1180	1398	1651	1931
	445	1011	1197	1420	1680	1965
	455	1023	1213	1443	1709	1998
	466	1035	1230	1466	1737	2031
	476	1046	1247	1488	1766	2064
	486	1058	1264	1511	1795	2096
	497	1070	1281	1534	1823	X
	507	1082	1298	1556	1851	X
	517	1094	1315	1579	1879	X

Table 6-4. Centerline Temperature for B = 0 MWd/kgUO_2

B = 75 MWd/kgUO_2						
Centerline Temp. (K)		Fuel radius (mm)				
		3	3.5	4	4.5	5
q''' (MW/m^3)	414	1056	1253	1485	1748	2026
	424	1069	1271	1510	1778	2060
	435	1082	1290	1535	1809	2094
	445	1096	1309	1560	1839	X
	455	1110	1328	1585	1869	X
	466	1123	1347	1609	1899	X
	476	1137	1366	1634	1928	X
	486	1150	1385	1659	1958	X
	497	1164	1404	1684	1986	X
	507	1178	1423	1708	2015	X
	517	1191	1442	1732	2043	X

6.6 Value for Constant Thermal Conductivity

Based on the HPR findings, this model determined how to produce a temperature profile for a constant thermal conductivity assumption. One unique product of this is the following: based on fuel size, heat generation rate, and burnup value, the value for constant thermal conductivity that will accurately predict the centerline temperature is determined. This information can be useful when in-pile instrumentation is not practical.

The following tables list the constant thermal conductivity value for various combinations of fuel parameters. These tables were produced with a surface temperature of 623K, however, the model can be modified to run for any surface temperature. The fuel also needs to be in thermal equilibrium. Once again, values are left out where the centerline temperature exceeded the upper limit given by [11] for BWR.

Table 6-5. Suggested Constant Thermal Conductivity for B = 0 MWd/kgUO_2

B = 0 MWd/kgUO_2								
Suggested Constant k (W/m-K)		Fuel radius (mm)						
		3	3.5	4	4.5	5	5.5	6
q''' (MW/m^3)	414	3.60	3.45	3.30	3.13	2.97	2.82	2.69
	424	3.59	3.44	3.28	3.12	2.95	2.80	2.68
	435	3.58	3.43	3.27	3.10	2.93	2.78	2.66
	445	3.57	3.41	3.25	3.08	2.91	2.76	2.65
	455	3.56	3.40	3.23	3.06	2.89	2.74	2.64
	466	3.55	3.39	3.22	3.04	2.87	2.73	X
	476	3.54	3.38	3.20	3.03	2.86	2.71	X
	486	3.53	3.36	3.19	3.01	2.84	2.70	X
	497	3.52	3.35	3.17	2.99	2.82	2.69	X
	507	3.51	3.34	3.16	2.98	2.81	2.67	X
	517	3.50	3.33	3.14	2.96	2.79	2.66	X

Table 6-6. Suggested Constant Thermal Conductivity for *B* = 25 $MWd/kgUO_2$

B = 25 $MWd/kgUO_2$							
Suggested Constant k (W/m-K)		Fuel radius (mm)					
		3	3.5	4	4.5	5	5.5
q''' (MW/m^3)	414	2.71	2.61	2.52	2.42	2.33	2.26
	424	2.70	2.60	2.51	2.41	2.32	2.26
	435	2.69	2.60	2.50	2.40	2.31	2.25
	445	2.69	2.59	2.49	2.39	2.30	2.25
	455	2.68	2.58	2.48	2.38	2.29	2.24
	466	2.67	2.57	2.47	2.37	2.29	X
	476	2.67	2.56	2.46	2.36	2.28	X
	486	2.66	2.56	2.45	2.35	2.27	X
	497	2.65	2.55	2.44	2.34	2.27	X
	507	2.65	2.54	2.43	2.33	2.26	X
	517	2.64	2.53	2.42	2.32	2.26	X

Table 6-7. Suggested Constant Thermal Conductivity for B = 50 MWd/kgUO_2

B = 50 MWd/kgUO_2						
Suggested Constant k (W/m-K)		Fuel radius (mm)				
		3	3.5	4	4.5	5
q''' (MW/m^3)	414	2.18	2.12	2.06	2.01	1.97
	424	2.18	2.12	2.06	2.00	1.97
	435	2.18	2.11	2.05	2.00	1.97
	445	2.17	2.11	2.05	1.99	1.97
	455	2.17	2.10	2.04	1.99	1.97
	466	2.16	2.10	2.03	1.99	1.97
	476	2.16	2.09	2.03	1.98	1.97
	486	2.15	2.09	2.02	1.98	1.97
	497	2.15	2.08	2.02	1.98	X
	507	2.15	2.08	2.02	1.97	X
	517	2.14	2.07	2.01	1.97	X

Table 6-8. Suggested Constant Thermal Conductivity for B = 75 MWd/kgUO$_2$

B = 75 MWd/kgUO$_2$						
Suggested Constant k (W/m-K)		Fuel radius (mm)				
		3	3.5	4	4.5	5
q''' (MW/m^3)	414	1.84	1.80	1.77	1.75	1.75
	424	1.84	1.80	1.77	1.75	1.76
	435	1.84	1.80	1.77	1.75	1.76
	445	1.83	1.80	1.76	1.75	X
	455	1.83	1.79	1.76	1.75	X
	466	1.83	1.79	1.76	1.75	X
	476	1.83	1.79	1.76	1.75	X
	486	1.82	1.78	1.75	1.75	X
	497	1.82	1.78	1.75	1.75	X
	507	1.82	1.78	1.75	1.75	X
	517	1.82	1.78	1.75	1.75	X

CHAPTER 7

HIGHER ORDER CORRELATIONS FOR THERMAL CONDUCTIVITY

7.1 HRP Correlation Discussion

In order to extract a data set for thermal conductivity that was a function of both temperature and burnup, it was necessary for HRP to impose simplifying assumptions. The data collected was centerline temperature, fuel surface temperature, and heat generation rate. In order to obtain a value for thermal conductivity from this type of data set, HRP assumed that the profile in the fuel rod was based on the constant thermal conductivity solution. Then the effective thermal conductivity was related to a temperature by Eq. (27).

$$(T,k)_0 = \left(\frac{T_0 + T_s}{2}, \frac{q''' \, r^2}{4(T_0 - T_s)}\right) \tag{27}$$

This data set introduces another point of error. The average of the temperature profile assumes that the profile was linear instead of using the constant thermal conductivity profile to extract the thermal conductivity value. This equation could be corrected by instead making a data set using the formulas in Eq. (28).

$$(T,k)_0 = \left(\frac{2T_0 + T_s}{3}, \frac{q''' \, r^2}{4(T_0 - T_s)}\right) \tag{28}$$

By changing the coolant temperature, or surface temperature, at a particular burnup value, the thermal conductivity can be determined as a function of temperature and burnup.

7.2 HRP Correlation Error

In order to investigate the error associated with the data set determined by HRP using Eq. (27) which resulted in the thermal conductivity correlation found in Eq. (1), the following method was used.

1- A hypothetical data set was generated, that, when placed in Eq. (27) would result in the HRP correlation result.

2- Instead of assuming that the profile in the fuel had constant thermal conductivity, the thermal conductivity that HRP determined as a function of temperature and burnup was used.

3- After solving the temperature profile for this particular case using the Kirchoff Transformation solution, the radius averaged temperature and thermal conductivity were used to generate a new data set (see Equation 29).

$$(T,k)_1 = \left(\frac{1}{r_s}\int_0^{r_s} T_{Kir}\,(r)dr, \frac{1}{r_s}\int_0^{r_s} k_{Kir}\,(T_{Kir})dr\right) \tag{29}$$

4- This data set $[(T,k)_1]$ was then compared to the original data set $[(T,k)_0]$, to determine the error.

5- By fitting the new data set, and repeating steps 2-4 (remembering to incorporate subscripts of the next iteration), the new data set can be shown to converge.

In accordance with step 1, the data set that was generated for this example is found in Table 7-1.

Table 7-1. Hypothetical Data Set Determined by Temperature Profile Model

T_{HRP} (K)	k_{HRP} (W/m-K)	ΔT (K)
673	4.70	600
823	4.02	701.8
973	3.52	801.8
1123	3.14	898.9
1273	2.85	991.7
1423	2.62	1078.1
1573	2.44	1155.6
1723	2.31	1220.6

Using the Kirchoff transformation solution to solve for the temperature profile, the radius averaged temperature and thermal conductivity can be found by Equation 29. This new data set is improved from the original because it assumes that thermal conductivity is a function of temperature and burnup, and not constant. This new data set can be found in Table 7-2.

Figure 7-1 suggests that there is a significant difference between the two results for thermal conductivity. Table 7-3 shows the error between the two data sets to be about 5%.

By fitting this new data set, a new correlation can be determined for thermal conductivity. The fit in Figure 7-2 is based on the same form of equation determined by HRP. This makes the solution simple, since the Kirchoff transformation solution still applies, except that the constants are different.

By using the same process to determine the average temperature and thermal conductivity values, a new data set of order $(T, k)_2$ can be determined. This new data set can be compared with the previous data sets to show that the correlation for thermal conductivity has effectively converged (difference between k_1 and k_2 is <1%), and that the overall HRP correlation error is approximately 6%.

Table 7-2. Temperature Values Correlated to Thermal Conductivity for k_1 Data Set

T_1 (K)	**k_1 (W/m-K)**
744.0	4.56
906.7	3.90
1069.5	3.42
1232.7	3.06
1396.3	2.79
1560.3	2.58
1724.6	2.44
1889.2	2.34

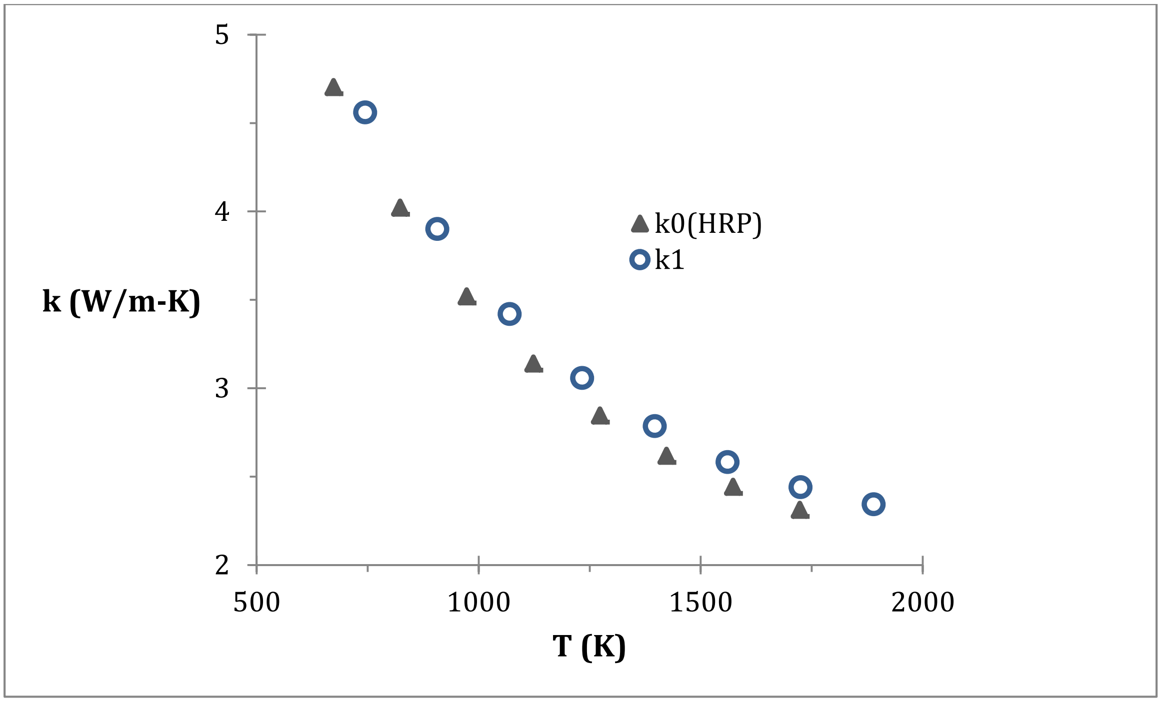

Figure 7-1. Hypothetical data sets for thermal conductivity (k_0 and k_1).

Table 7-3. Percentage Difference Between k_0 and k_1 Data Sets at Various Temperatures

T (K)	Error (%)
744.0	4.56
906.7	4.56
1069.5	4.56
1232.7	4.61
1396.3	4.72
1560.3	4.95
1724.6	5.31
1889.2	**5.39**

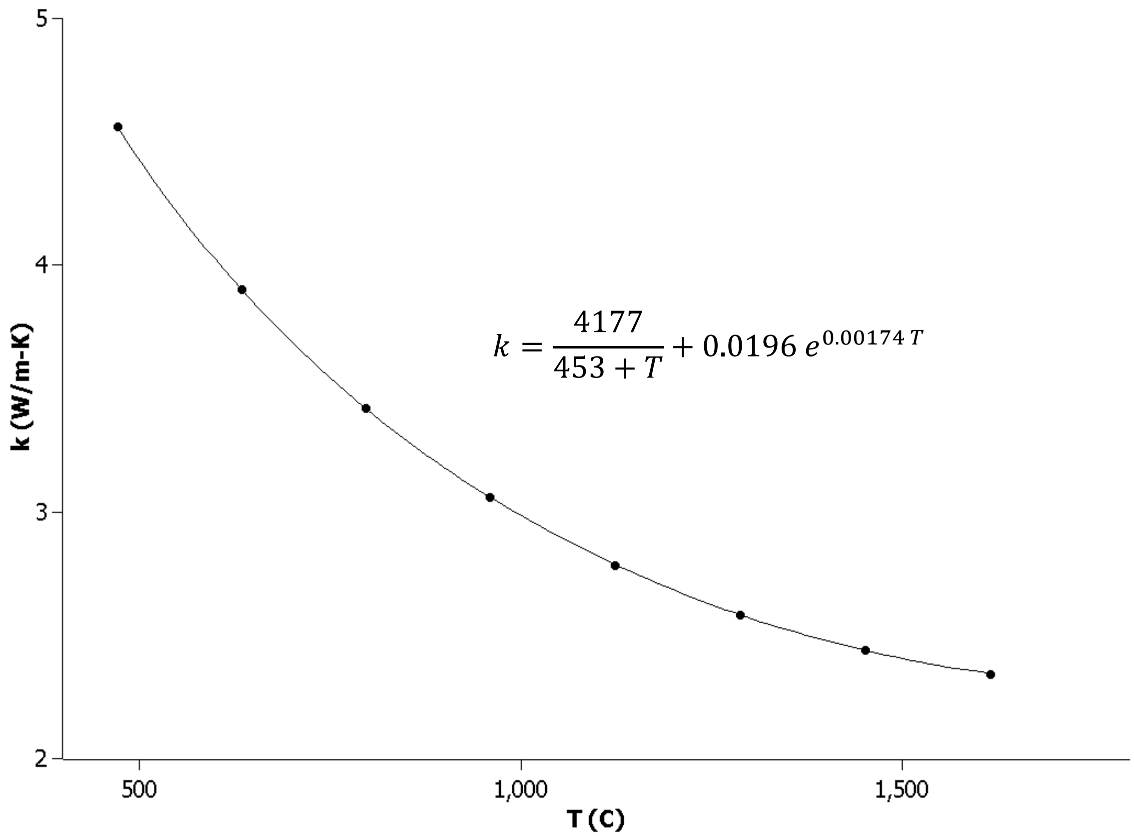

Figure 7-2. Fitting plot and function for data set k_1.

Table 7-4. Temperature Values Correlated to Thermal Conductivity for k_2 Data Set

T_2 (K)	k_2 (W/m-K)
741.3	4.59
904.3	3.94
1066.7	3.45
1229.6	3.09
1392.8	2.82
1556.4	2.61
1720.3	2.44
1884.5	2.35

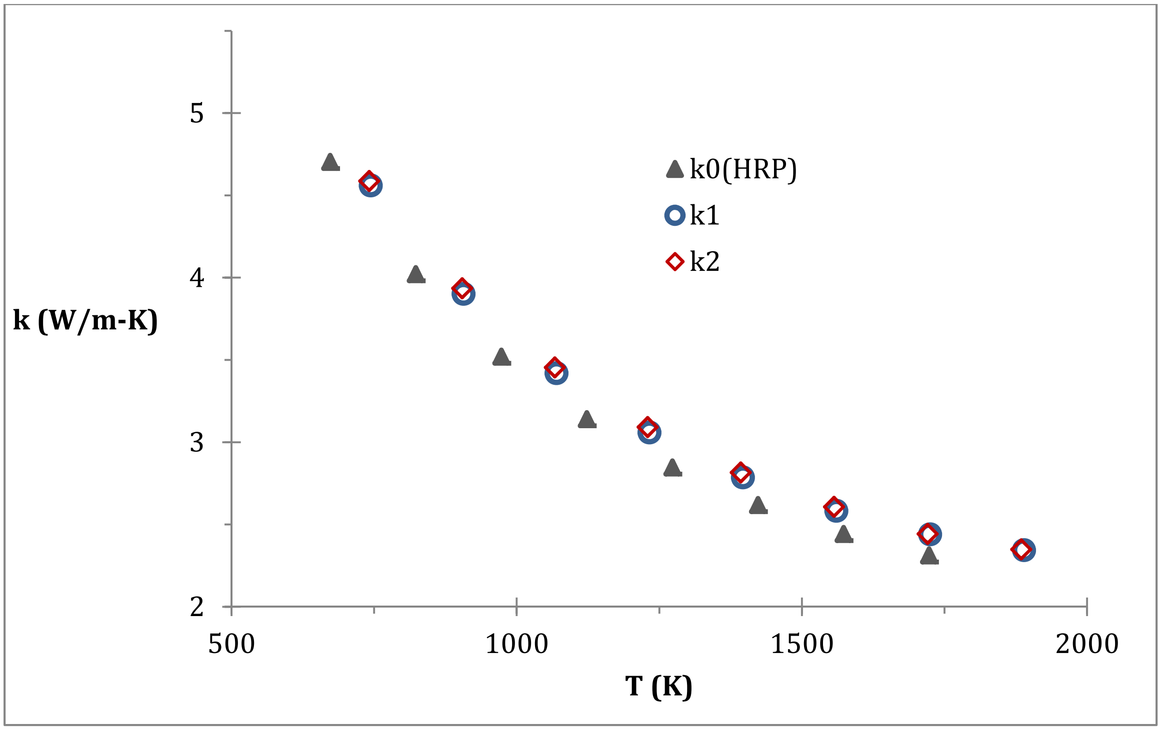

Figure 7-3. Hypothetical data sets for thermal conductivity (k_0, k_1, and k_2).

Table 7-5. Percentage Difference Between k_0 and k_2 Data Sets at Various Temperatures

T (K)	**Error (%)**
741.3	4.84
904.3	5.17
1066.7	5.29
1229.6	5.42
1392.8	5.56
1556.4	**5.63**
1720.3	5.25
1884.5	5.45

Table 7-6. Percentage Difference Between k_1 and k_2 Data Sets at Various Temperatures

T (K)	Error (%)
741.3	0.20
904.3	0.61
1066.7	0.73
1229.6	0.79
1392.8	0.79
1556.4	0.68
1720.3	0.05
1884.5	0.03

7.3 Determining Higher Order Correlations for Thermal Conductivity

A general data processing procedure has been identified to aid in future two thermocouple experiments for measuring in-pile thermal conductivity. This procedure can be applied to data taken by the same method used by HRP. The data processing procedure can be summarized in the following steps:

1- Obtain in-pile data using two thermocouple method. In particular, collect values for centerline temperature, surface temperature, heat generation rate, and burnup.
2- Impose a temperature profile in the fuel using the constant thermal conductivity assumption to extract values for temperature and thermal conductivity. Use Equation 28 to extract particular values.
3- Fit the data with a correlation of the form determined by HRP. The form of the equation to be used can be found in Eq. (1).
4- Using the correlation found in step 3 for thermal conductivity, assume that the temperature profile is a function of this new expression for thermal conductivity.

5- Use the Kirchoff Transformation solution to solve for the temperature profile in the fuel rod.

6- Take the radius averaged temperature and thermal conductivity to construct a new higher order data set. Use Eq. (29) to construct this data set.

7- Determine the improvement by comparing the error, or difference, between the data set of step 6 and the data set of step 2.

8- Fit the data set of step 6 with a correlation of the form Eq. (1) similar to step 3.

9- If the error, or difference, between the data sets is significantly small, the correlation is converging and further iteration may not be necessary. If the error is large, assume that the temperature profile is a function of the thermal conductivity correlation found in step 8, and repeat steps 5-9.

CHAPTER 8

SUMMARY AND CONCLUSIONS

Understanding the error associated with the constant thermal conductivity assumption allows development of more accurate thermal conductivity correlations. These correlations can be developed through future in-pile measurements or by using the HRP data. Conclusions of this study:

- For a burnup value of 0 MWd/kgUO_2, an error as great as 12% in the temperature profile was determined, assuming constant thermal conductivity. As burnup value increases, the error decreases. Therefore, in the cases of higher burnup values of 25, 50 and 75 MWd/kgUO_2, errors were determined as high as 8%, 5%, and 3%, respectively.
- Fuel radius seems to be the main effect contributing to the magnitude of the temperature error within the fuel rod. Heat generation has a relatively small effect on the magnitude of the error. However, heat generation and fuel radius together determine the overall error of the constant thermal conductivity assumption.
- The effect of processing the data using an iterative method to determine higher order correlations showed that the difference in thermal conductivity of a higher order correlation from the original HRP correlation is about 6%.
- The data processing method outlined is a useful way to obtain a more accurate correlation for thermal conductivity than that presented by HRP.

CHAPTER 9

FUTURE WORK

This report outlines the following work to be done on this subject:

- Using the data processing method introduced in this report, reprocess the data collected by HRP. This would result in a more accurate correlation for thermal conductivity in UO_2 fuel. This has not been accomplished as part of the report due to the unavailability of the HRP data.
- Incorporate the data processing method in reactors with similar measurement techniques, like those being accomplished at the Massachusetts Institute of Technology.

REFERENCES

[1] Hofman, G.L., and Kim, Y.S., "A Classification of Uniquely Different Types of Nuclear Fission Gas Behavior," *Nuclear Engineering and Technology*, Vol. 37, No. 4, Aug. 2005, pp. 299-308.

[2] Solstad, S., and Nieuwenhove, R.V., "Instrument Capabilities and Developments at the Halden Reactor Project," *Proceedings of the 6th ANS NPIC HMIT 2009 Topical Meeting on Nuclear Plant Intrumentation Controls, and Human Machine Interface Technology*, Knoxville, TN, April 2009.

[3] Fox, Brandon S., "In-Pile Thermal Conductivity Measurement Methods for Nuclear Fuels" (2010). *All Graduate Theses and Dissertations.* Paper 660. http://digitalcommons.usu.edu/etd/660

[4] Wiesenack, W., and Tverberg, T., "The OECD Halden Rector Project Fuels Testing Programme: Selected Results and Plans," *Nuclear Engineering and Design*, Vol. 207, No. 2, April 2001, pp. 189-197.

[5] Tverberg, T., "In-Pile Fuel Rod Performance Characterization in the Halden Reactor," *Technical Meeting on "Fuel Rod Instrumentation and In-Pile Measurement Techniques*," Halden, Norway, Sept. 2007.

[6] Khandelwal, M., and Mench, M.M., "Direct measurement of through-plane thermal conductivity and contact resistance in fuel cell materials," *Journal of Power Sources*, Vol. 161, No. 2, Oct. 2006, pp. 1106-1111.

[7] Beckwith, T.G., Marangoni, R.D., and Lienhard V, J.H., *Mechanical Measurements: Sixth Edition*, Pearson: Prentice Hall, Upper Saddle, NJ, 2007, pp. 34-43.

[8] Cezairliyan, A., "Survey of Measurement Techniques," *Compendium* of *Thermophysical Property Measurement Methods,* Vol. 1, Plenum Press, New York, 1984, pp. 169-230.

[9] Touloukian, Y. S., Powell, R. W., Ho, C. Y., and Klemens P. G., editors, *Thermal Conductivity,* Thermophysical Properties of Matter, Vol. 1, Plenum Press, New York, NY, Feb.1970, pp. 1-8.

[10] Presley, M. A., and Christensen, P. R., "Thermal Conductivity Measurements of Particulate Materials," *Journal of Geophysical Research*, Vol. 102, No. 3, March 1997, pp. 6535-6549.

[11] Nero, A. V. Jr., *A Guidebook to Nuclear Reactors*, University of California Press, Ltd., London, England, 1979.

[12] Rust, J. H., *Nuclear Power Plant Engineering*, Haralson Publishing Company, Buchanan, GA, 1979.

[13] Todreas, N. E., and Kazimi, M. S., *Nuclear Systems I - Thermal Hydraulic Fundamentals*, Hemisphere Publishing Corporation, New York, NY, 1990.

[14] Incropera, F.P., Dewitt, D.P., Bergman, T.L., and Lavine, A.S., *Fundamentals of Heat and Mass Transfer: Sixth Edition*, John Wiley and Sons, New York, NY, 2007.

[15] Jiji, L.M., *Heat Conduction: Third Edition*, Springer, New York, NY, 2009, pp. 215-224.

[16] Chapra, S.C., and Canale, R.P., *Numerical Methods for Engineers: Fifth Edition*, McGraw Hill, New York, NY, 2006, pp. 139-145.

APPENDICES

Appendix A: Results of Various Burnup Parameters for One Case

In order to see the full effects on error, this appendix is provided for one fuel type over burnup values of 0, 25, 50, and 75 MWd/kgUO_2. The heat generation rate is 466 MW/m^3. The radius of the fuel is 4.5mm. The surface temperature is 623K.

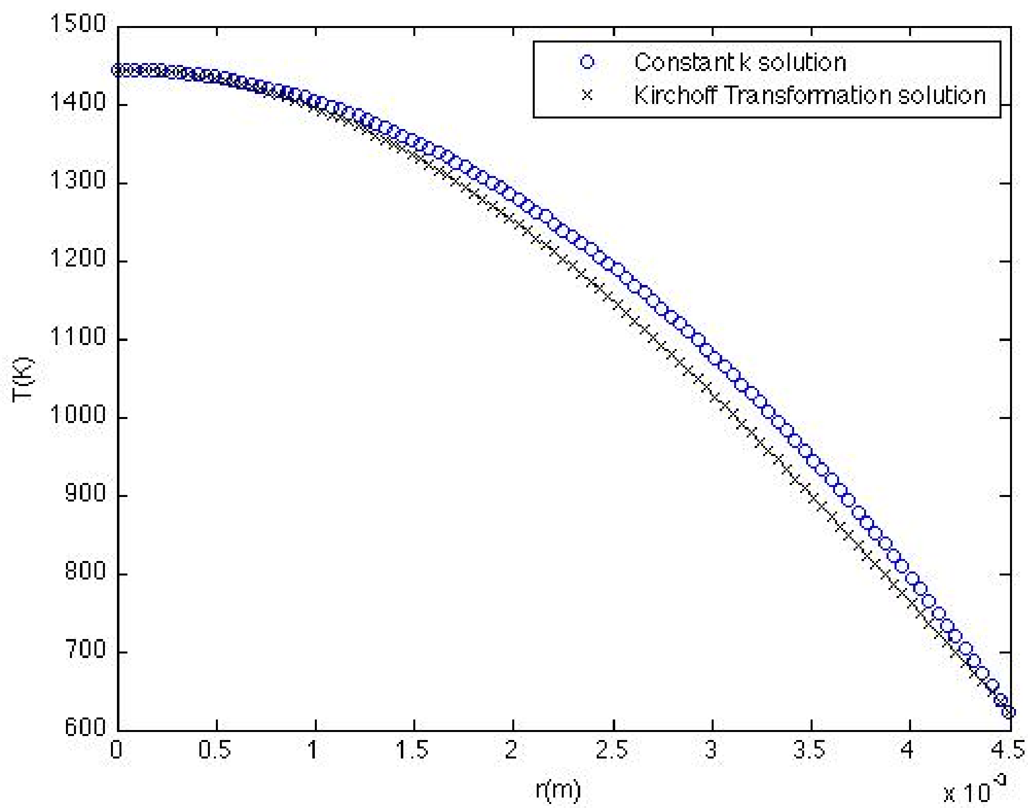

Figure A-1. Temperature profile solutions for B = 0 MWd/kgUO_2.

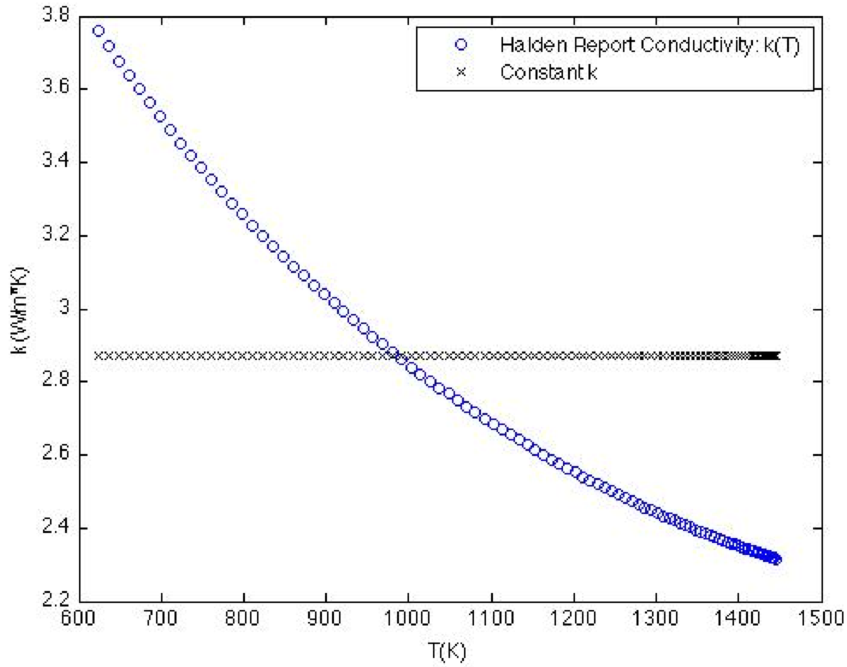

Figure A-2. Thermal conductivity plot against temperature for $B = 0$ MWd/kgUO$_2$.

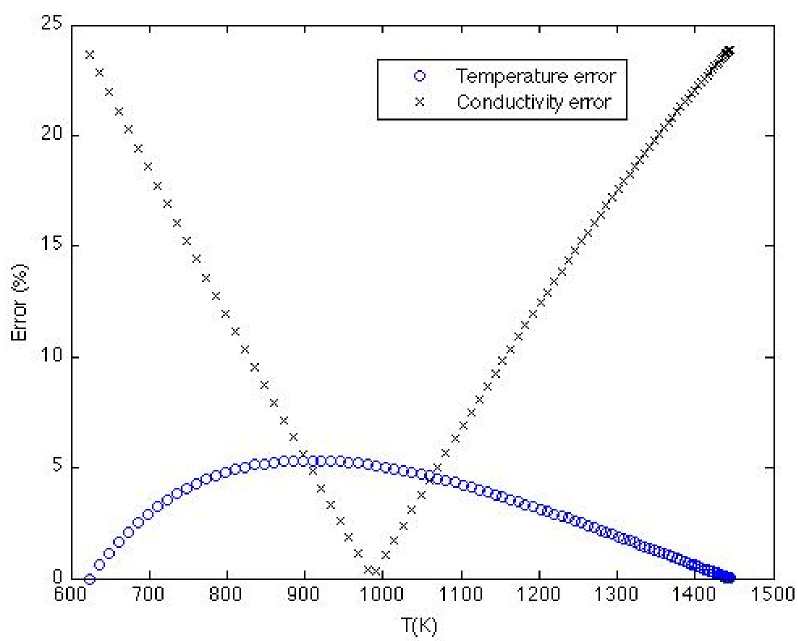

Figure A-3. Error of constant thermal conductivity assumption against temperature for $B = 0$ MWd/kgUO$_2$.

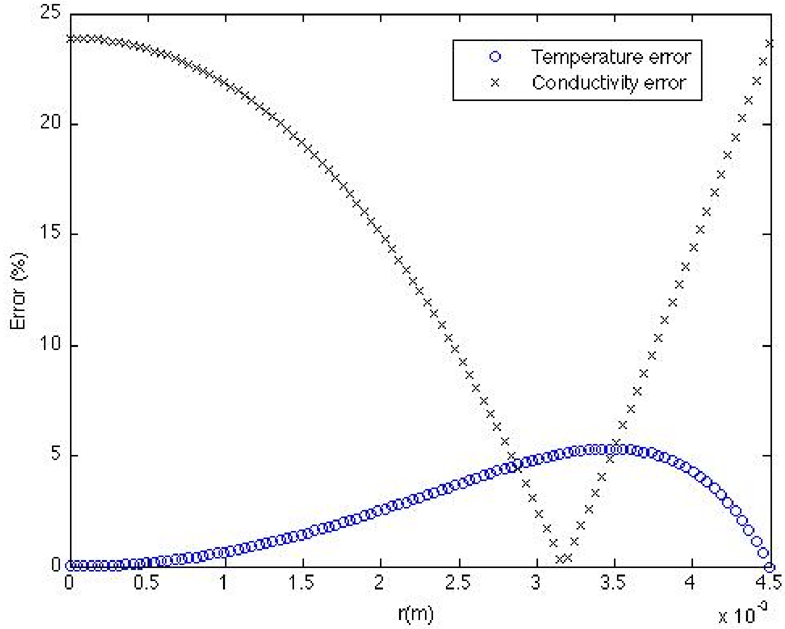

Figure A-4. Error of constant thermal conductivity assumption against radius for $B = 0$ MWd/kgUO$_2$.

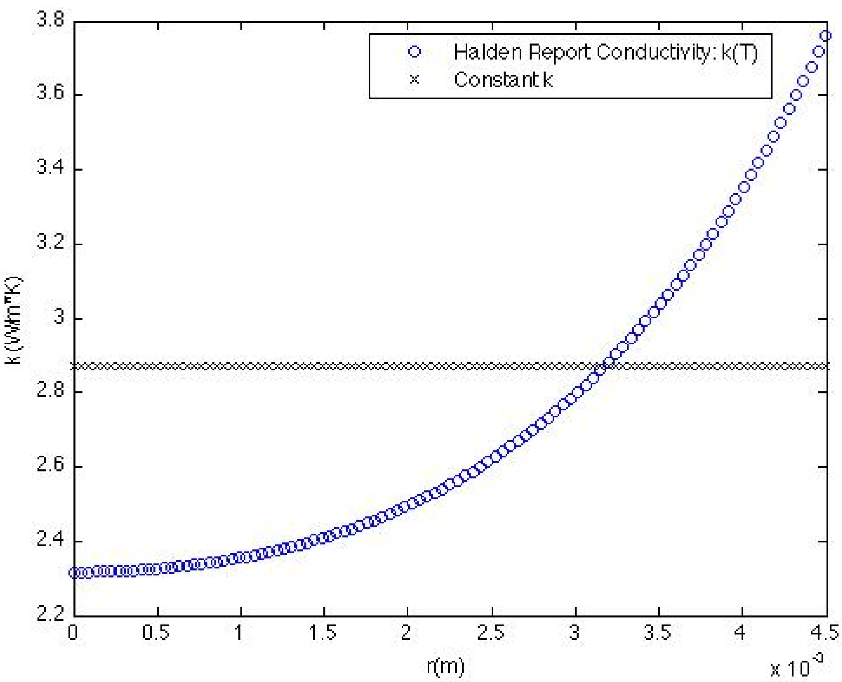

Figure A-5. Thermal conductivity plot against radius for $B = 0$ MWd/kgUO$_2$.

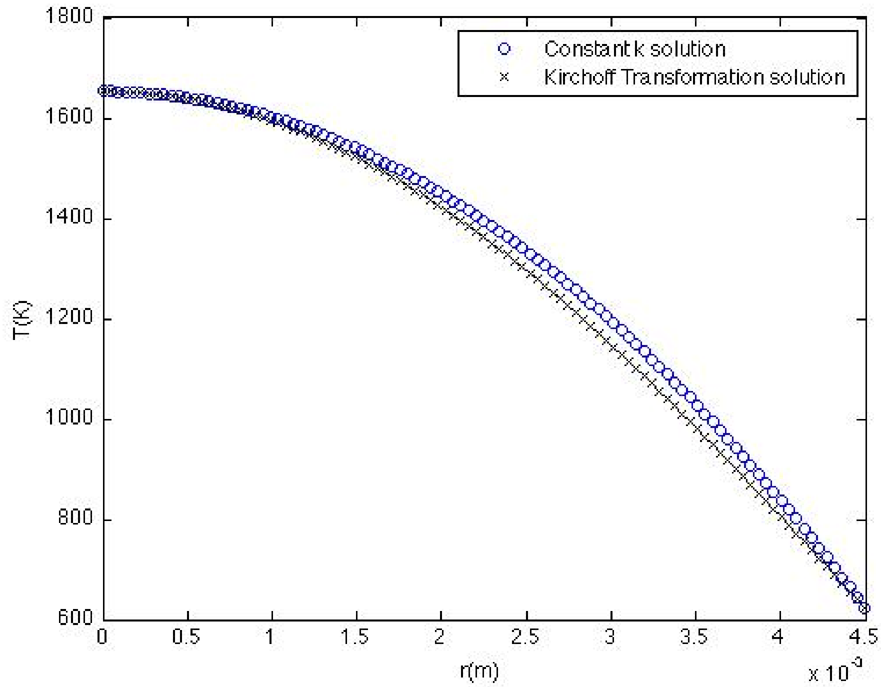

Figure A-6. Temperature profile solutions for B = 25 MWd/kgUO$_2$.

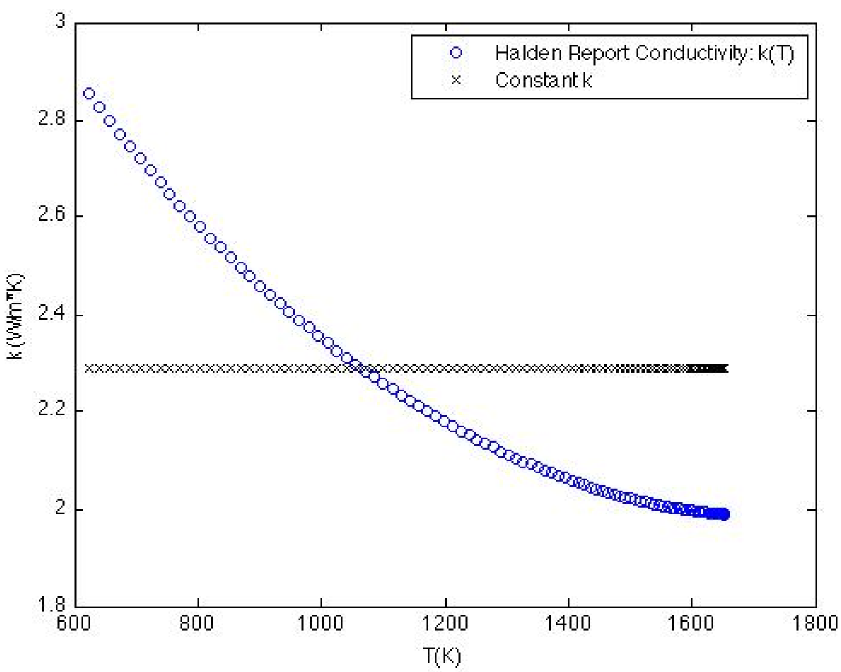

Figure A-7. Thermal conductivity plot against temperature for B = 25 MWd/kgUO$_2$.

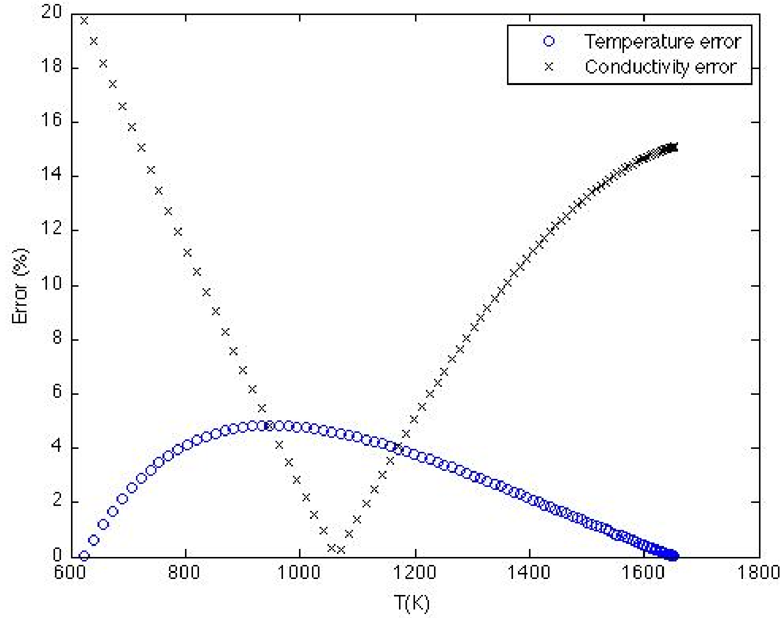

Figure A-8. Error of constant thermal conductivity assumption against temperature for *B* = 25 MWd/kgUO_2.

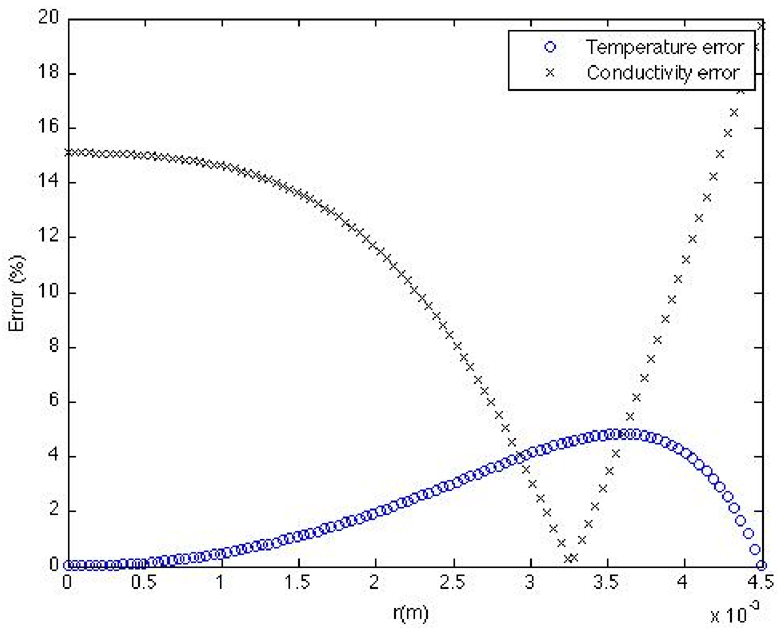

Figure A-9. Error of constant thermal conductivity assumption against radius for *B* = 25 MWd/kgUO_2.

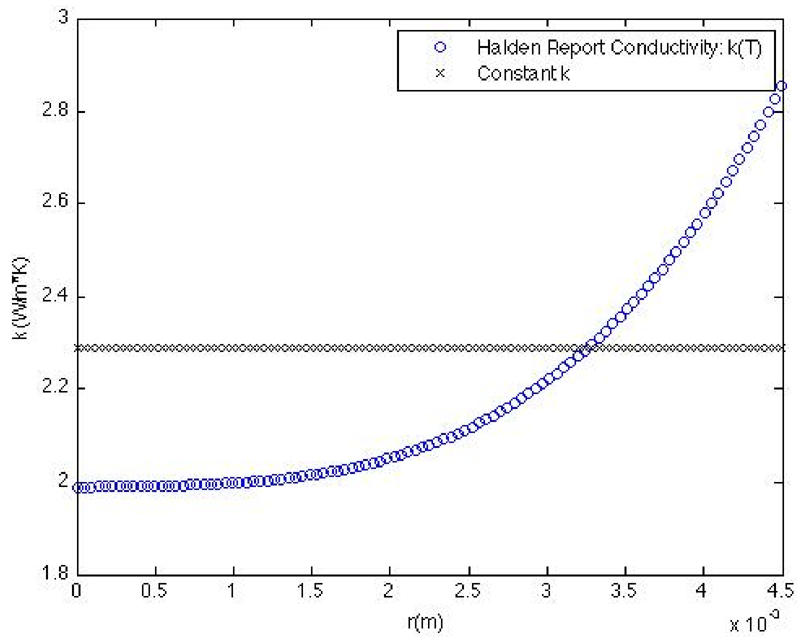

Figure A-10. Thermal conductivity plot against radius for B = 25 MWd/kgUO_2.

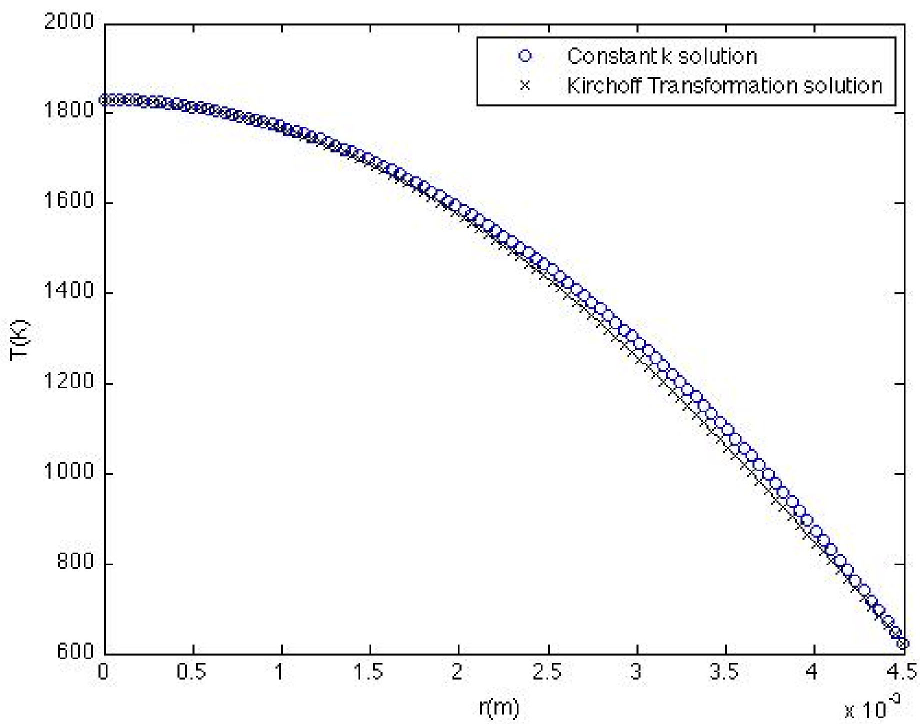

Figure A-11. Temperature profile solutions for B = 50 MWd/kgUO_2.

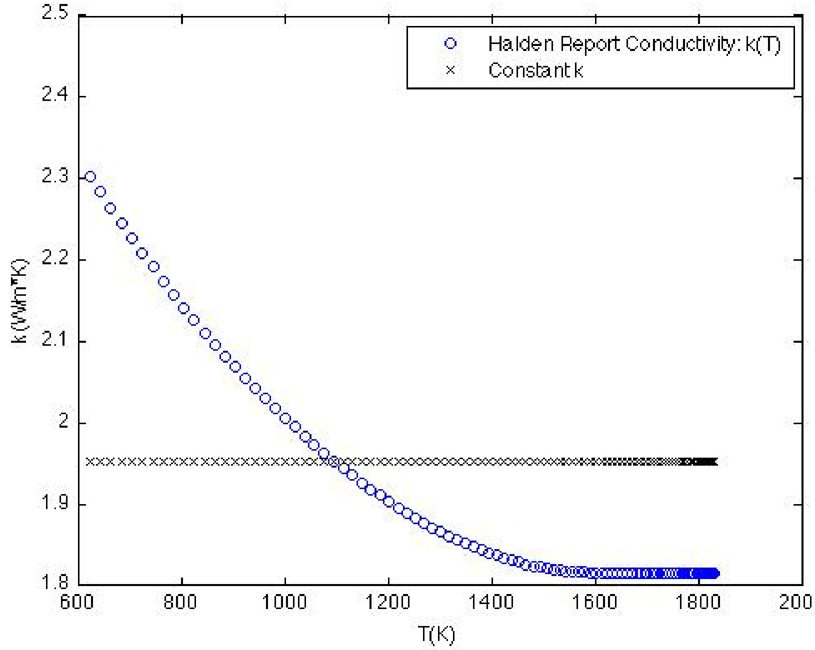

Figure A-12. Thermal conductivity plot against temperature for B = 50 MWd/kgUO$_2$.

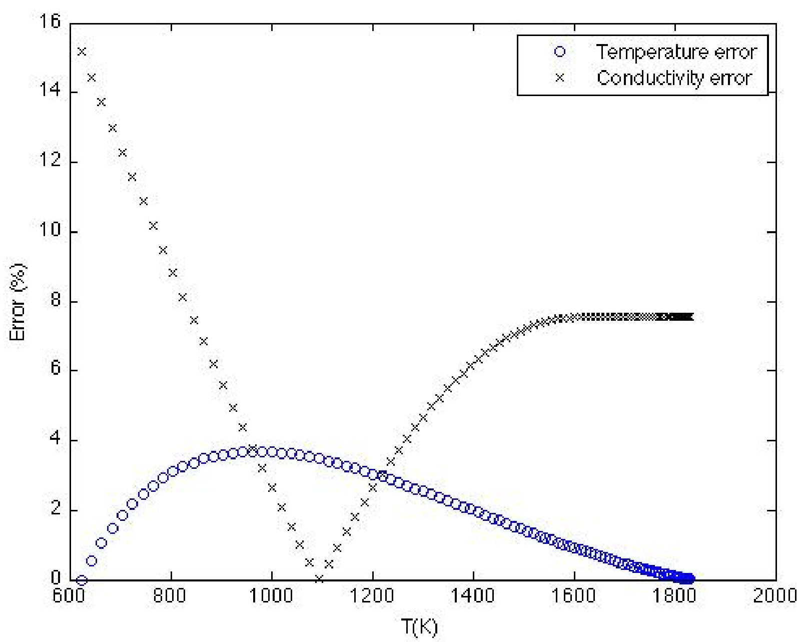

Figure A-13. Error of constant thermal conductivity assumption against temperature for B = 50 MWd/kgUO$_2$.

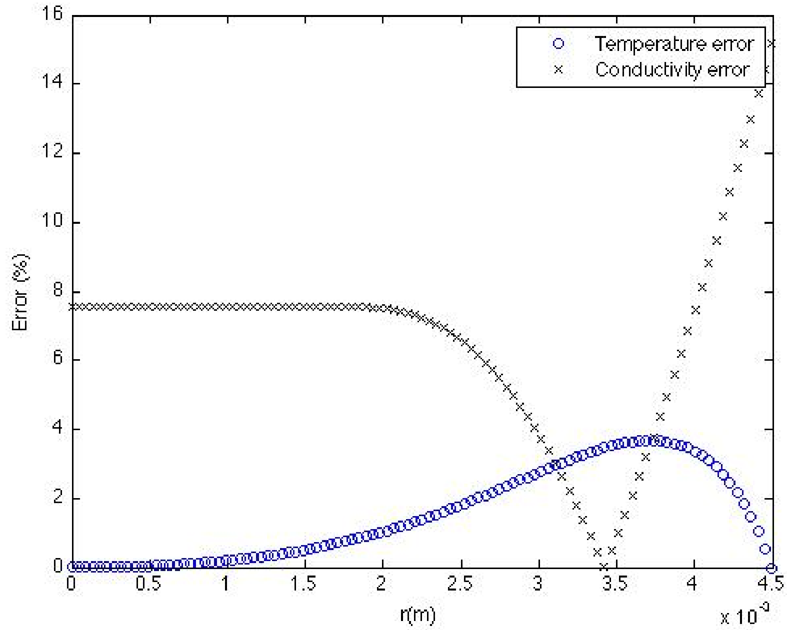

Figure A-14. Error of constant thermal conductivity assumption against radius for B = 50 MWd/kgUO$_2$.

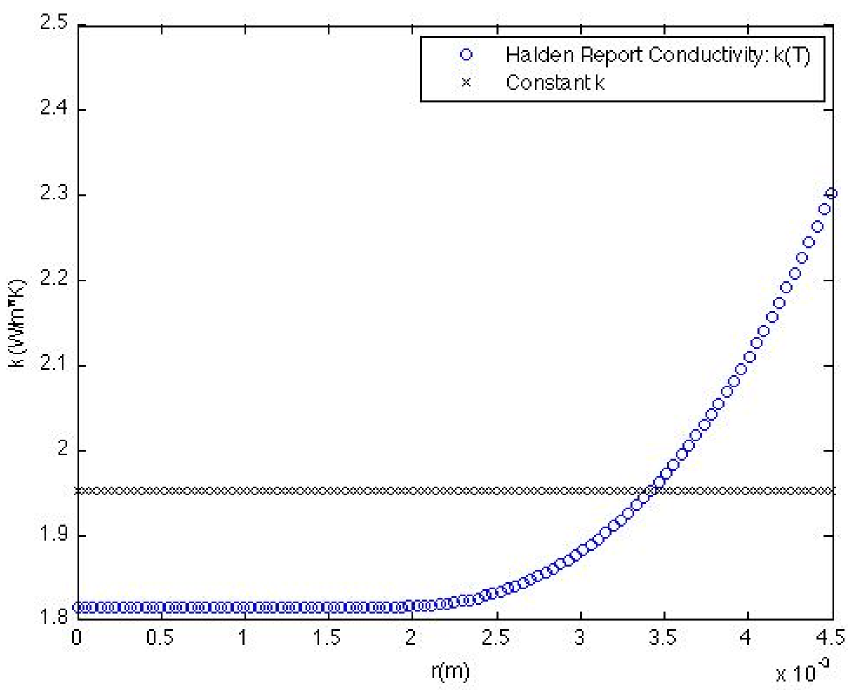

Figure A-15. Thermal conductivity plot against radius for B = 50 MWd/kgUO$_2$.

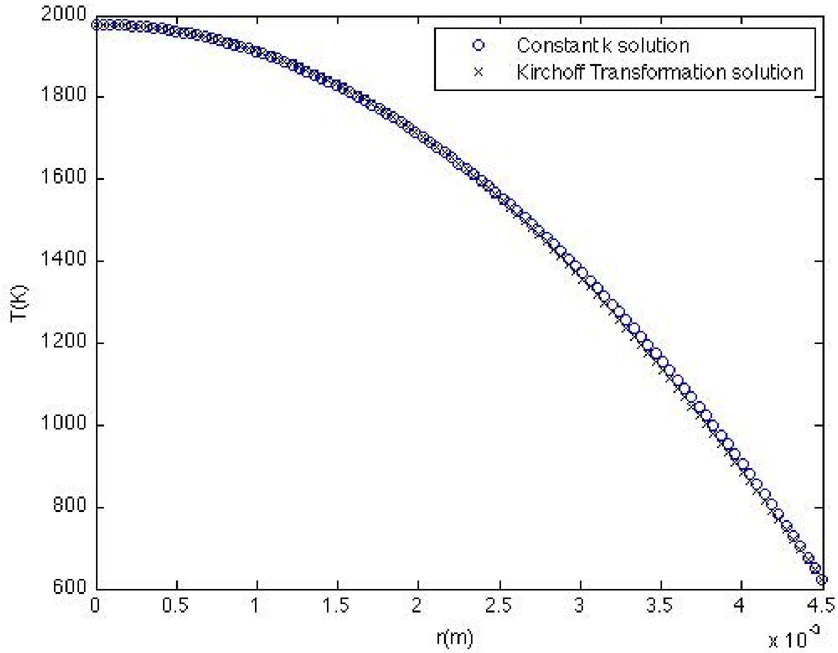

Figure A-16. Temperature profile solutions for B = 75 MWd/kgUO$_2$.

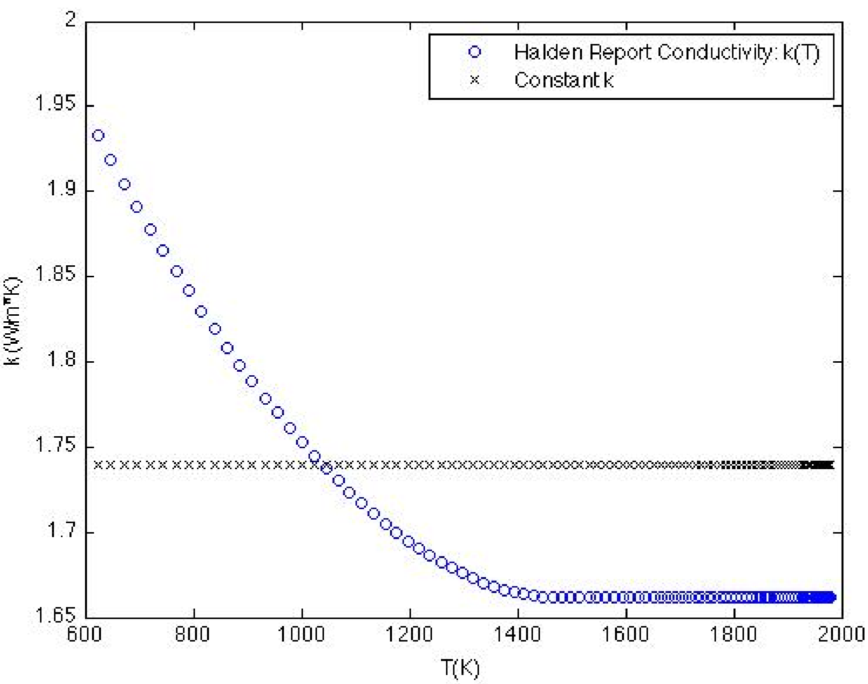

Figure A-17. Thermal conductivity plot against temperature for B = 75 MWd/kgUO$_2$.

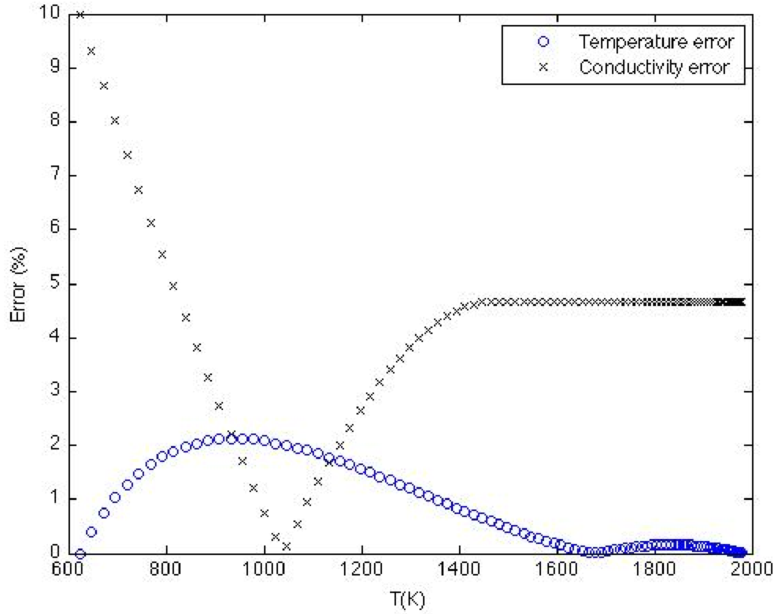

Figure A-18. Error of constant thermal conductivity assumption against temperature for *B* = 75 MWd/kgUO_2.

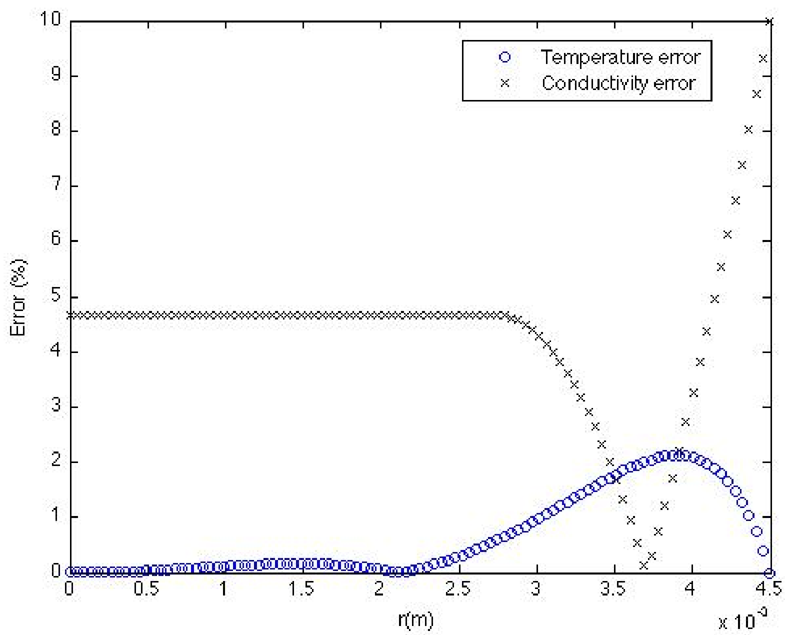

Figure A-19. Error of constant thermal conductivity assumption against radius for *B* = 75 MWd/kgUO_2.

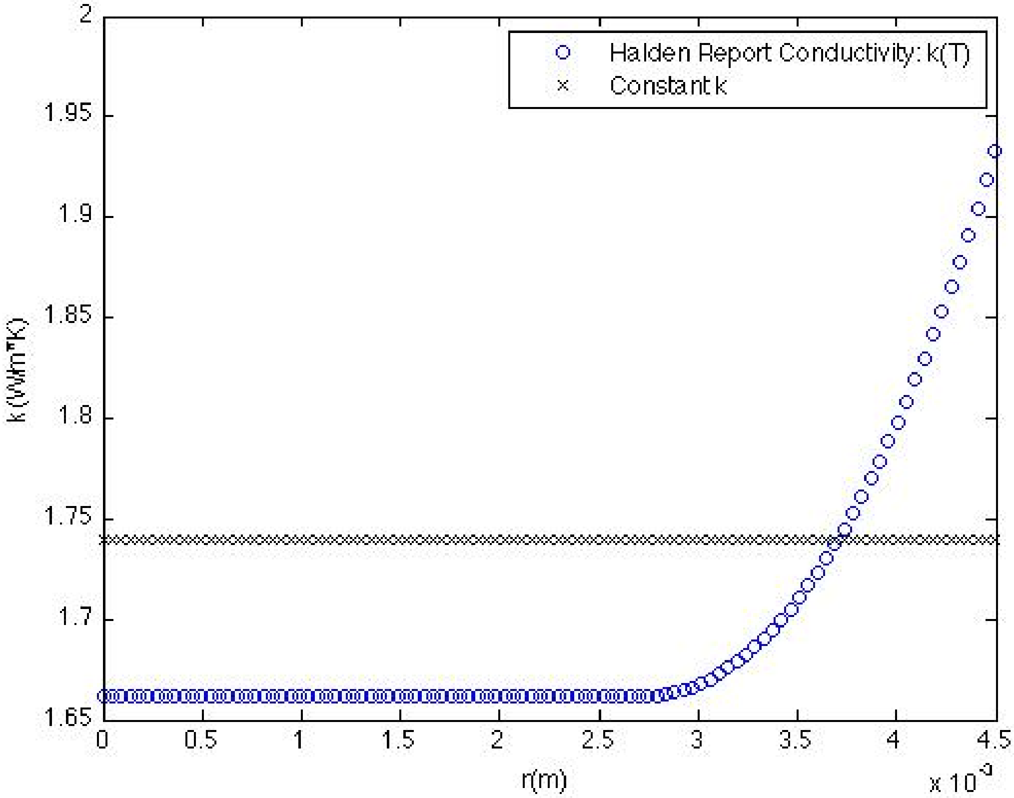

Figure A-20. Thermal conductivity plot against radius for B = 75 MWd/kgUO_2.

Appendix B: Effects of Heat Generation Rate and Radius for All Burnup Parameters

The following plots are listed in order to provide the reader with results of error over various heat generation rates and fuel radii. The figures cover burnup values of 0, 25, 50, and 75 MWd/kgUO$_2$. The surface temperature was kept constant at 623K.

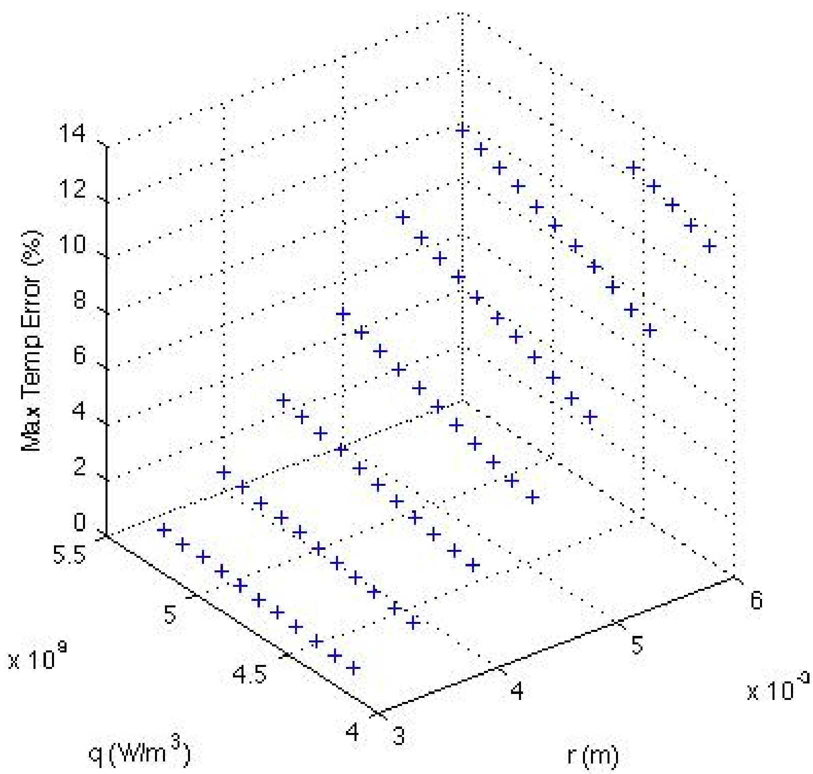

Figure B-1. Temperature error of constant thermal conductivity assumption for $B = 0$ MWd/kgUO$_2$ for various heat generation rates and fuel sizes.

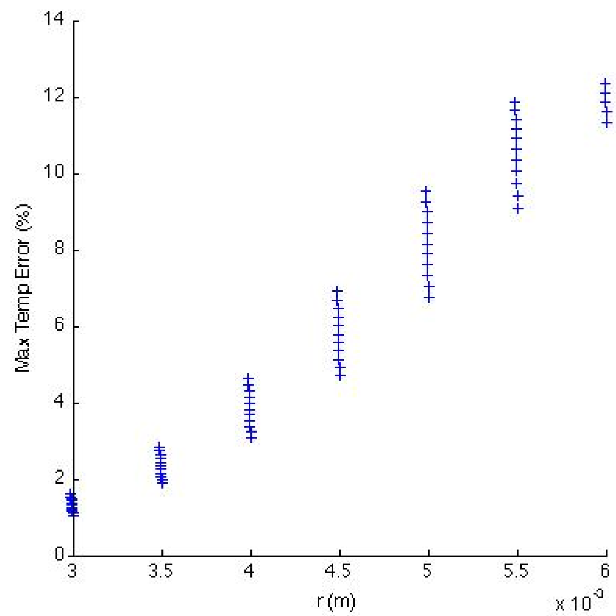

Figure B-2. Temperature error of constant thermal conductivity assumption for $B = 0$ MWd/kgUO_2 against fuel sizes.

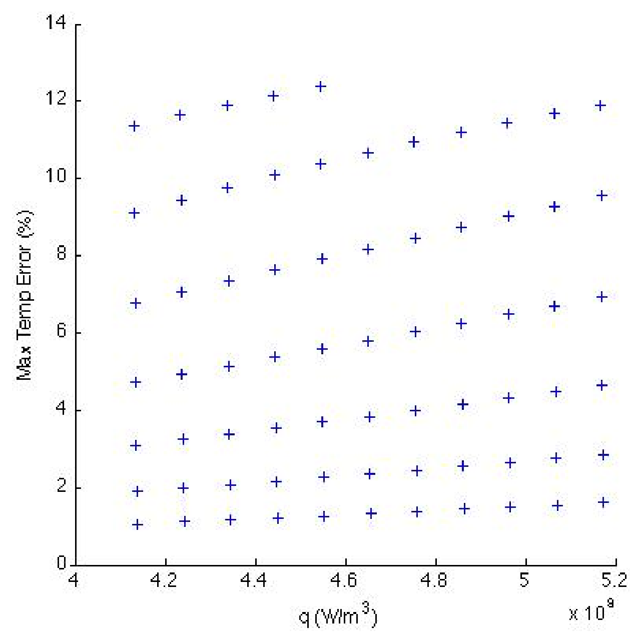

Figure B-3. Temperature error of constant thermal conductivity assumption for $B = 0$ MWd/kgUO_2 against heat generation rate.

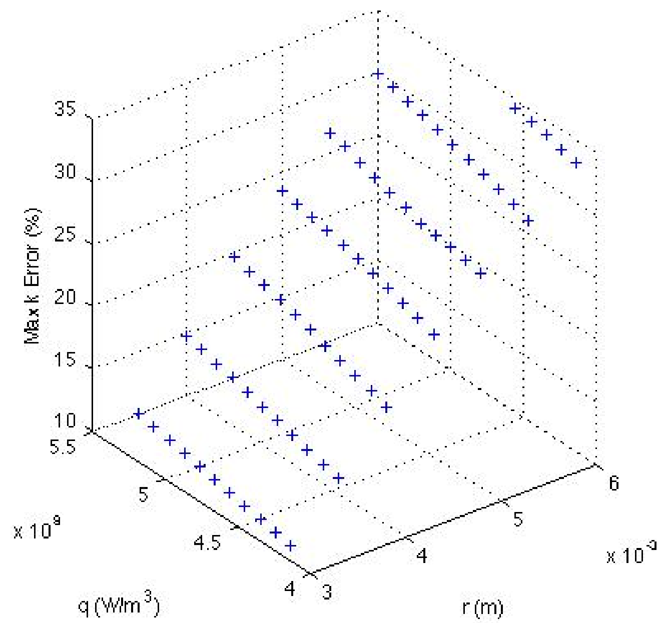

Figure B-4. Thermal conductivity error of constant thermal conductivity assumption for $B = 0$ MWd/kgUO_2 for various heat generation rates and fuel sizes.

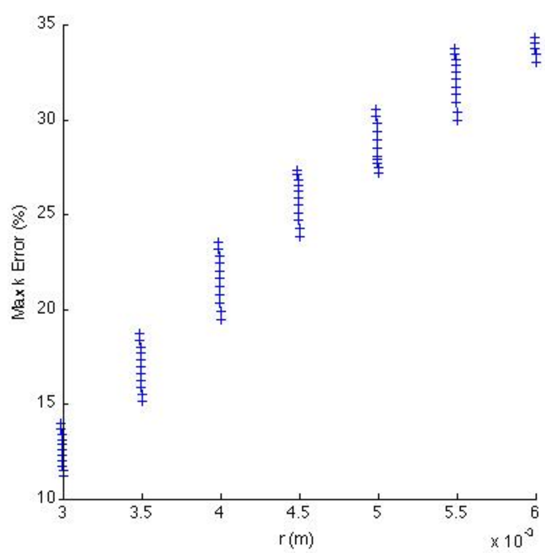

Figure B-5. Thermal conductivity error of constant thermal conductivity assumption for $B = 0$ MWd/kgUO_2 against fuel sizes.

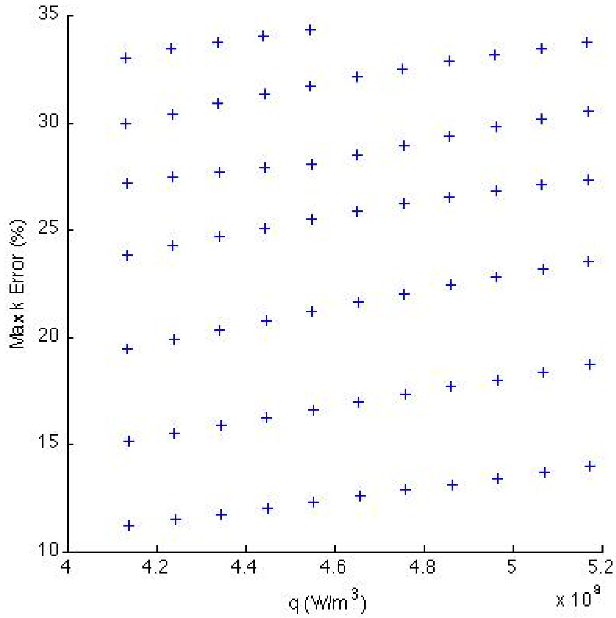

Figure B-6. Thermal conductivity error of constant thermal conductivity assumption for $B = 0$ MWd/kgUO$_2$ against heat generation rate.

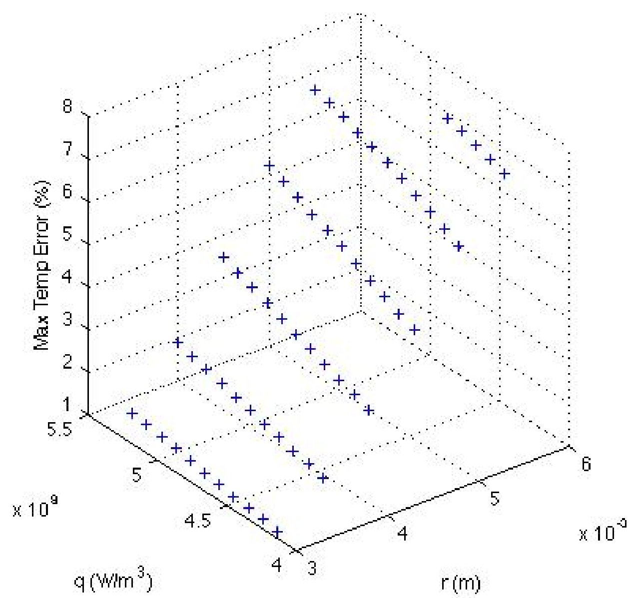

Figure B-7. Temperature error of constant thermal conductivity assumption for $B = 25$ MWd/kgUO$_2$ for various heat generation rates and fuel sizes.

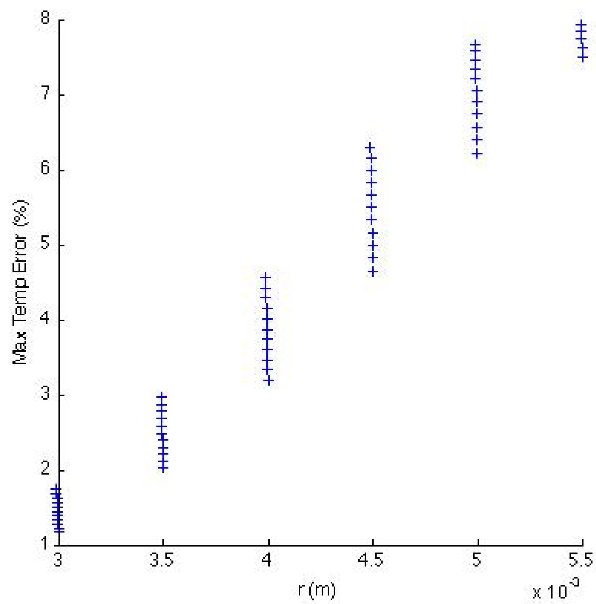

Figure B-8. Temperature error of constant thermal conductivity assumption for *B* = 25 MWd/kgUO_2 against fuel sizes.

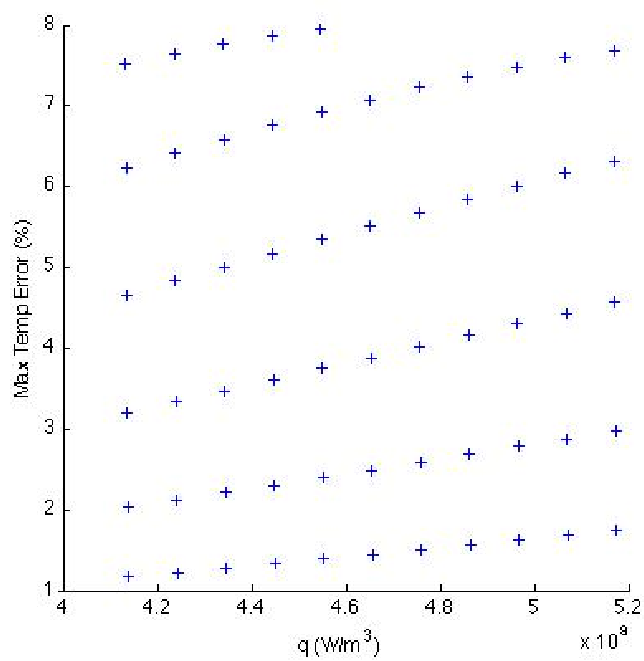

Figure B-9. Temperature error of constant thermal conductivity assumption for *B* = 25 MWd/kgUO_2 against heat generation rate.

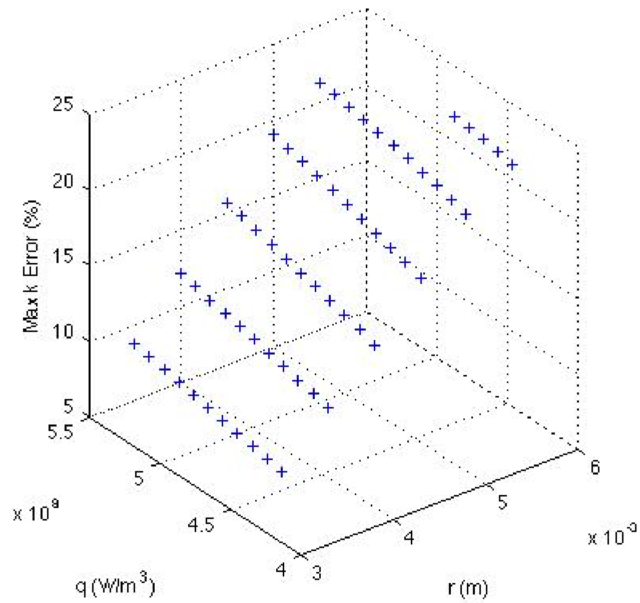

Figure B-10. Thermal conductivity error of constant thermal conductivity assumption for B = 25 MWd/kgUO_2 for various heat generation rates and fuel sizes.

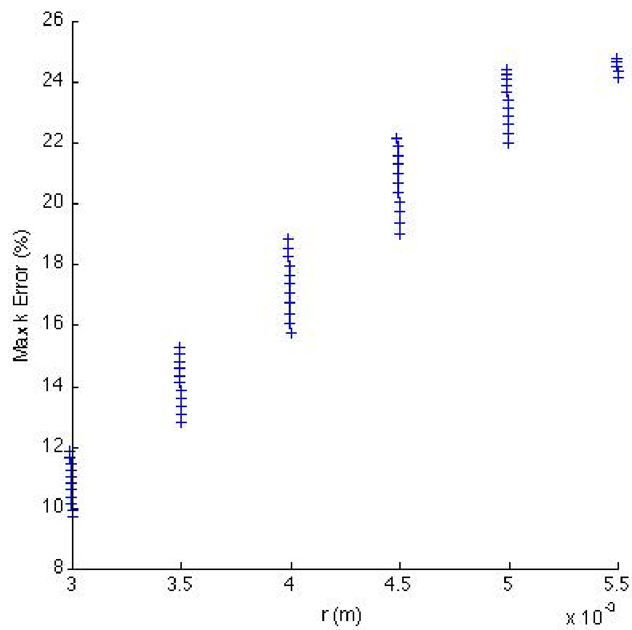

Figure B-11. Thermal conductivity error of constant thermal conductivity assumption for B = 25 MWd/kgUO_2 against fuel sizes.

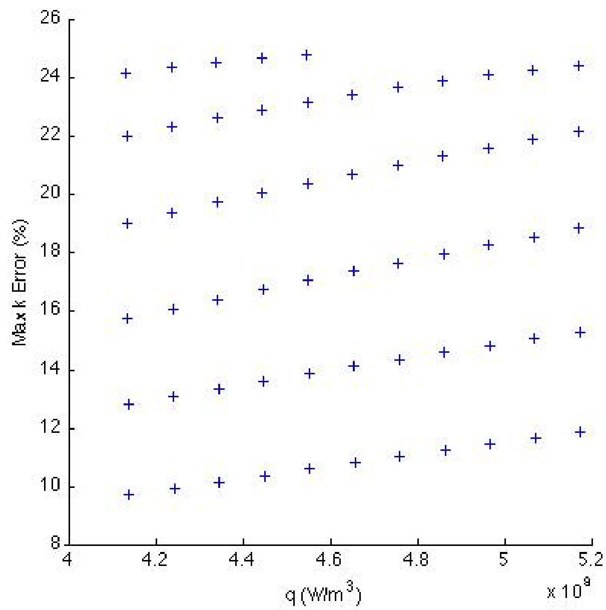

Figure B-12. Thermal conductivity error of constant thermal conductivity assumption for $B = 25$ MWd/kgUO_2 against heat generation rate.

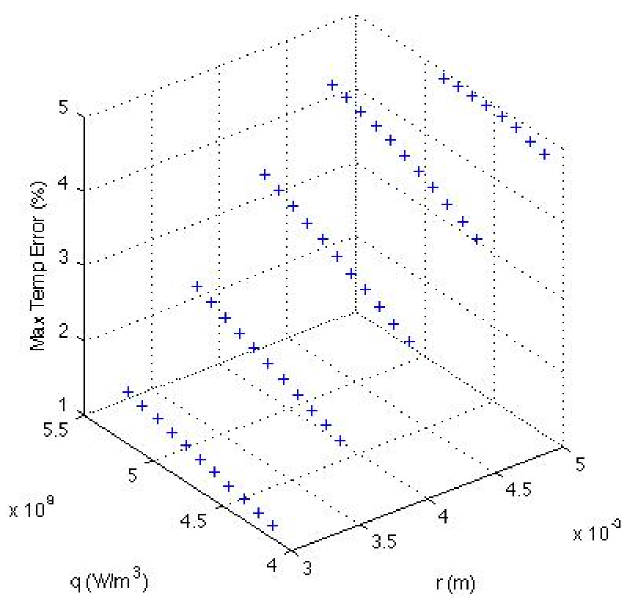

Figure B-13. Temperature error of constant thermal conductivity assumption for $B = 50$ MWd/kgUO_2 for various heat generation rates and fuel sizes.

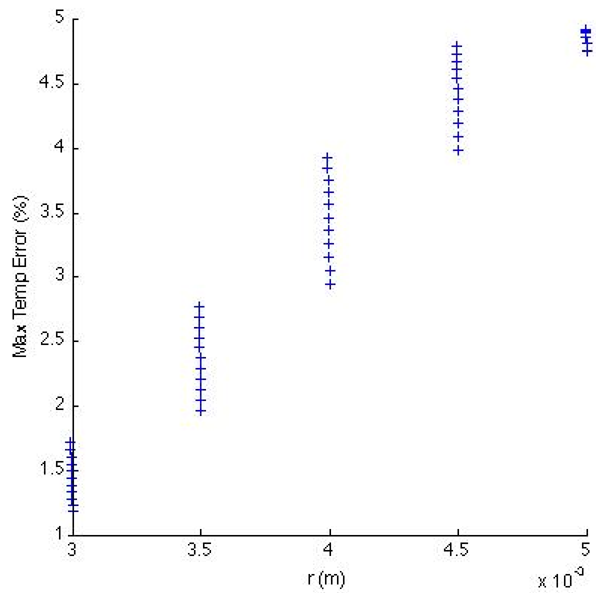

Figure B-14. Temperature error of constant thermal conductivity assumption for *B* = 50 MWd/kgUO_2 against fuel sizes.

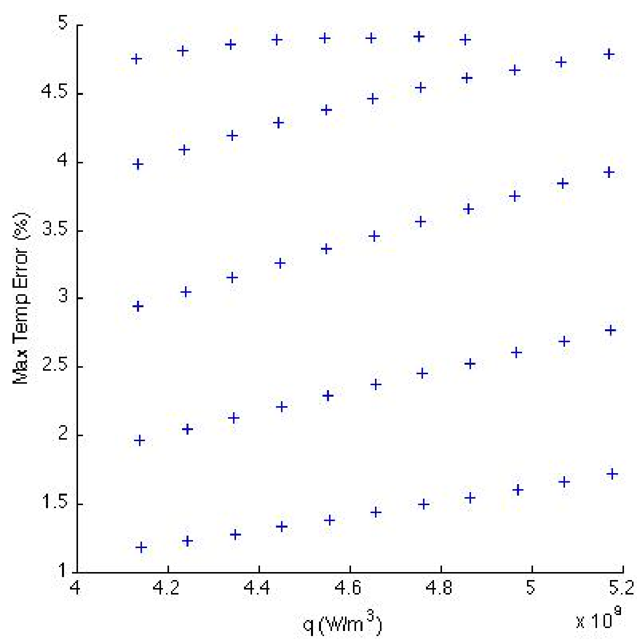

Figure B-15. Temperature error of constant thermal conductivity assumption for *B* = 50 MWd/kgUO_2 against heat generation rate.

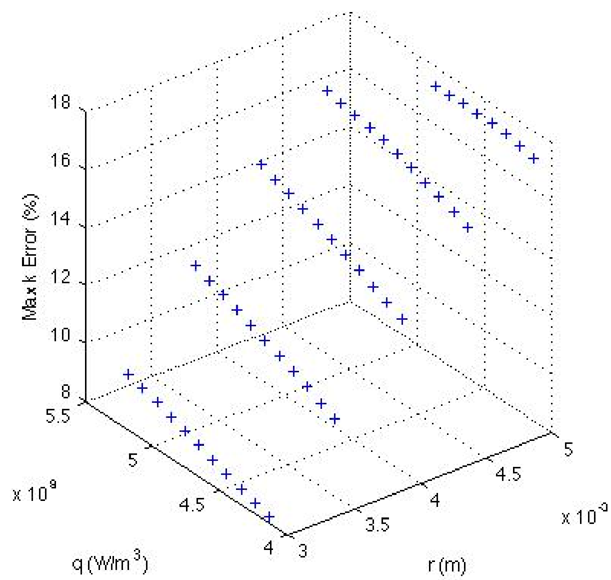

Figure B-16. Thermal conductivity error of constant thermal conductivity assumption for *B* = 50 MWd/kgUO_2 for various heat generation rates and fuel sizes.

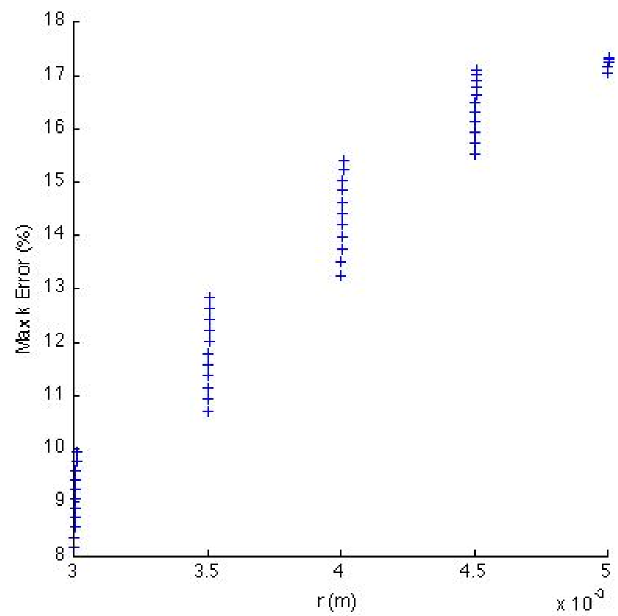

Figure B-17. Thermal conductivity error of constant thermal conductivity assumption for *B* = 50 MWd/kgUO_2 against fuel sizes.

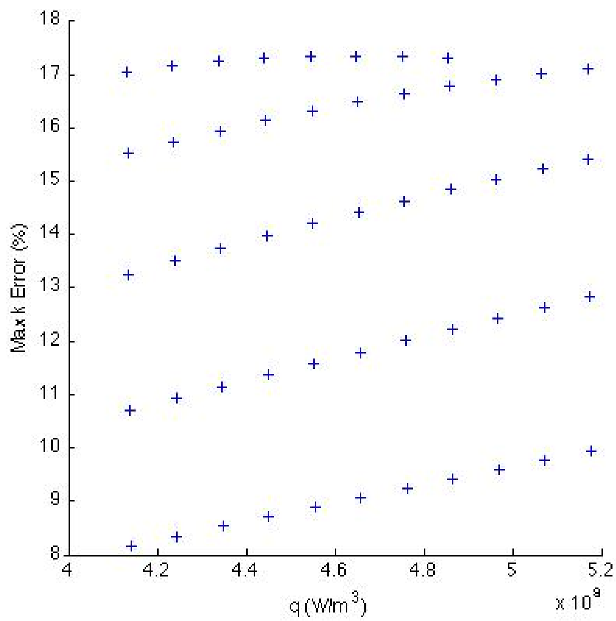

Figure B-18. Thermal conductivity error of constant thermal conductivity assumption for *B* = 50 MWd/kgUO$_2$ against heat generation rate.

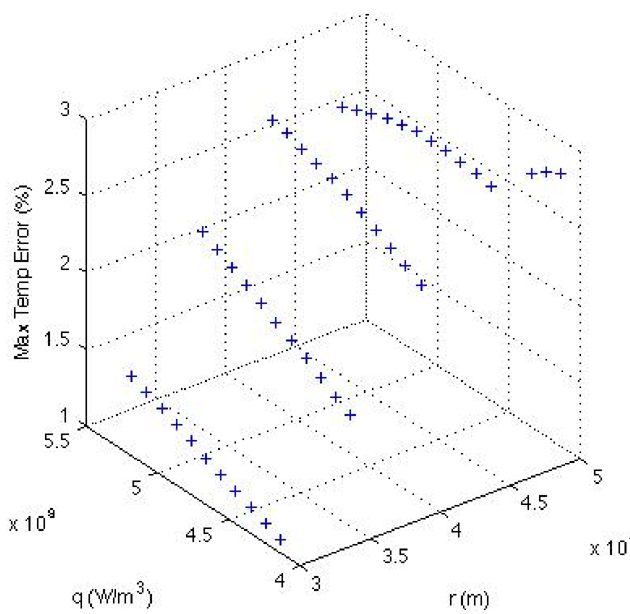

Figure B-19. Temperature error of constant thermal conductivity assumption for *B* = 75 MWd/kgUO$_2$ for various heat generation rates and fuel sizes.

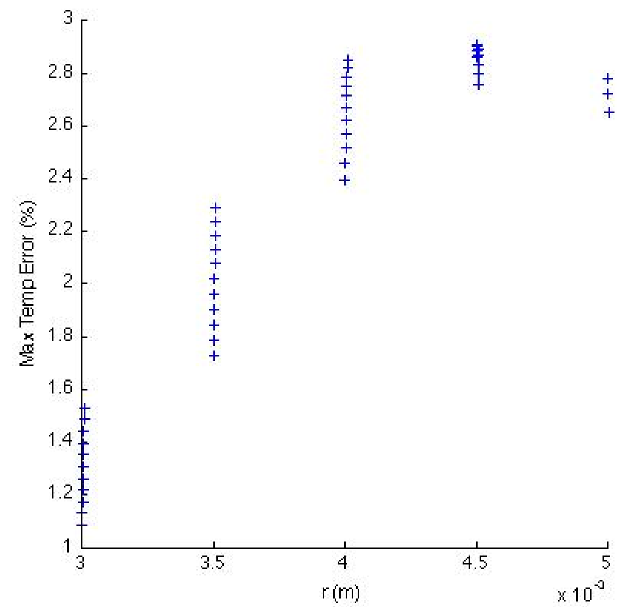

Figure B-20. Temperature error of constant thermal conductivity assumption for *B* = 75 MWd/kgUO_2 against fuel sizes.

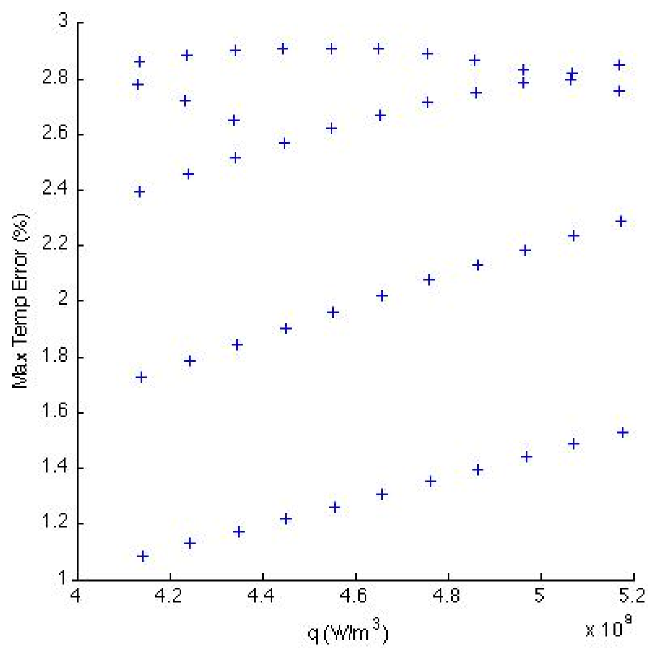

Figure B-21. Temperature error of constant thermal conductivity assumption for *B* = 75 MWd/kgUO_2 against heat generation rate.

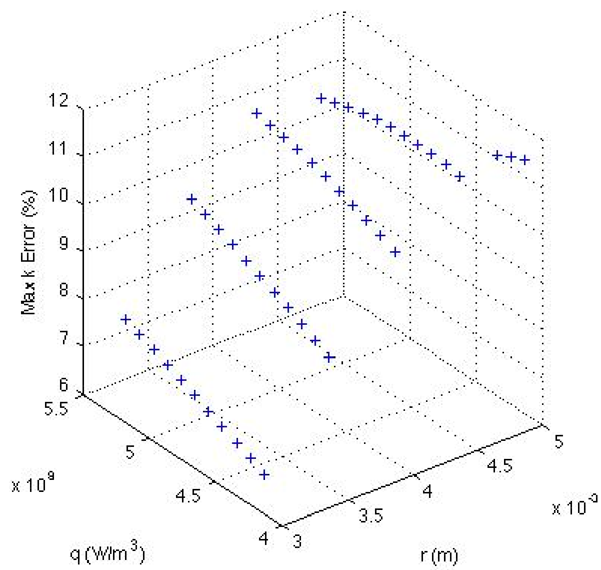

Figure B-22. Thermal conductivity error of constant thermal conductivity assumption for B = 75 MWd/kgUO_2 for various heat generation rates and fuel sizes.

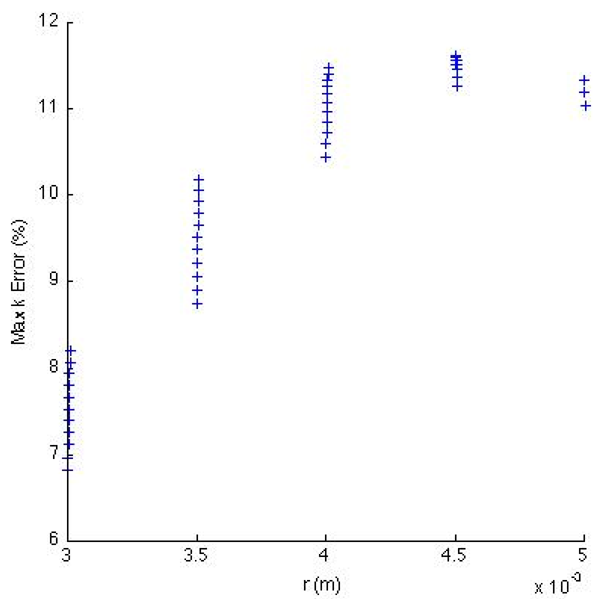

Figure B-23. Thermal conductivity error of constant thermal conductivity assumption for B = 75 MWd/kgUO_2 against fuel sizes.

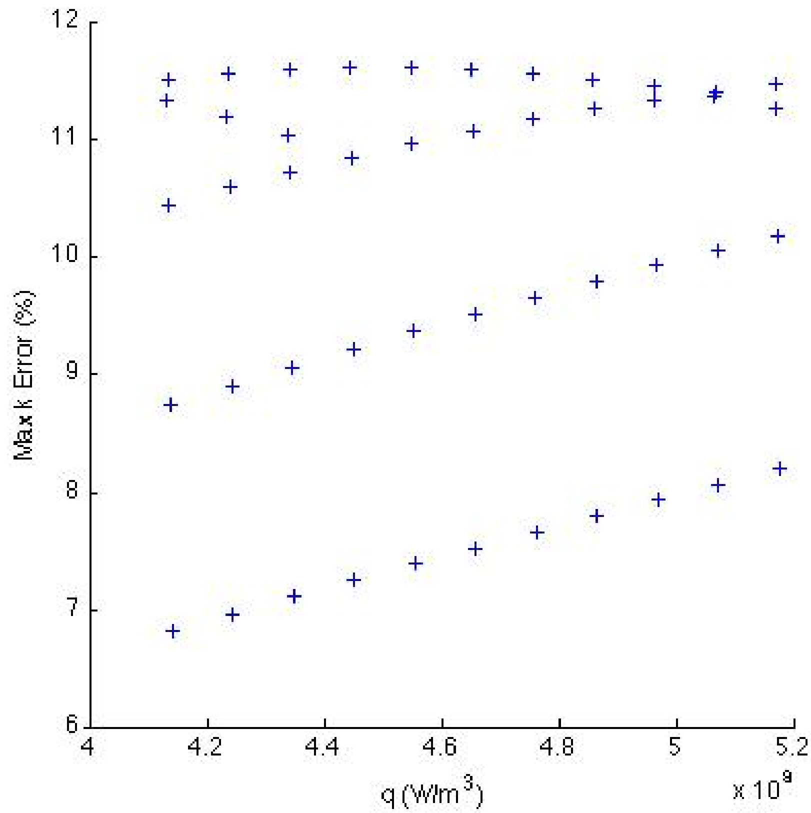

Figure B-24. Thermal conductivity error of constant thermal conductivity assumption for *B* = 75 MWd/kgUO_2 against heat generation rate.